A High Accuracy Vehicle Positioning System Implemented in a Lane Assistance System when GPS Is Unavailable

Final Report

Prepared by:

Edmund Arpin V
Craig Shankwitz
Max Donath

Department of Mechanical Engineering
Intelligent Vehicles Laboratory
University of Minnesota

CTS 11-18

Technical Report Documentation Page

1. Report No.	2.	3. Recipients Accession No.	
CTS 11-18			
4. Title and Subtitle A High Accuracy Vehicle Positioning System Implemented in a Lane Assistance System when GPS in Unavailable		5. Report Date July 2011 6.	
7. Author(s) Edmund Arpin V, Craig Shankwitz, Max Donath		8. Performing Organization Report No.	
9. Performing Organization Name and Address Intelligent Vehicles Laboratory Department of Mechanical Engineering 111 Church St. S.E. Minneapolis, MN 55455		10. Project/Task/Work Unit No. CTS Project #2007046 and #2008052 11. Contract (C) or Grant (G) No.	
12. Sponsoring Organization Name and Address Intelligent Transportation Systems Institute Center for Transportation Studies University of Minnesota 200 Transportation and Safety Building 511 Washington Ave. SE Minneapolis, MN 55455		13. Type of Report and Period Covered Final Report; Aug. 2006 – Sept. 2008 14. Sponsoring Agency Code	
15. Supplementary Notes http://www.its.umn.edu/Publications/ResearchReports/			

16. Abstract (Limit: 200 words)

The use of lane assistance systems can reduce the stress levels experienced by drivers and allow for better lane keeping in narrow, bus-dedicated lanes. In 2008, the Intelligent Vehicles (IV) Lab at the University of Minnesota has developed such a system for this purpose. The IV Lab lane-assist system uses dual frequency differential GPS (DGPS) for high accuracy position information. This position information is used in conjunction with a geospatial database containing the road geometry and lane boundary positions required for a lane-assistance system. In urban environments, where tall buildings, overpasses, and other obstructions to the sky are present, DGPS suffers from inaccuracies and outages. This report proposes a method for replacing DGPS sensing with a high accuracy vehicle positioning system which fuses data from RFID (Radio Frequency IDentification) and LiDAR (Light Detection and Ranging) curb detection.

A Vehicle Positioning System (VPS) was originally developed by the IV Lab to provide the lane level ("which lane on the road") position of a vehicle with respect to a known reference (i.e., a mile marker or start of roadway) by the use of encoded position information in RFID tags on the roadway, read by the vehicle. The lateral position resolution of VPS is constrained to one lane width, which is insufficient for lane-assistant systems. Thus, in-lane level ("where in the lane") lateral position estimation was supplemented by a LiDAR unit that generates an accurate position of the vehicle with respect to the curb, which is cross referenced with a map database that provides the distance from the lane center to the curb, thus providing the vehicle's lateral offset from the lane center. On-board odometry is used to maintain accurate longitudinal position in between tag reads. By fusing the information from the VPS, LiDAR, and on-board odometry, high accuracy, "where in lane" level vehicle positioning can be maintained from this enhanced VPS during DGPS outages.

17. Document Analysis/Descriptors	18. Availability Statement		
Lane guidance system, Lane assistance system, Route guidance, Driver assistance system, Driver support systems, RFID positioning system, Vehicle positioning system (VPS), Motorist aid systems, Radio frequency identification, Automatic vehicle location	No restrictions. Document available from: National Technical Information Services, Alexandria, Virginia 22312		
19. Security Class (this report)	20. Security Class (this page)	21. No. of Pages	22. Price
Unclassified	Unclassified	82	

A High Accuracy Vehicle Positioning System Implemented in a Lane Assistance System when GPS Is Unavailable

Final Report

Prepared by:

Edmund Arpin V
Craig Shankwitz
Max Donath

Department of Mechanical Engineering
Intelligent Vehicles Laboratory
University of Minnesota

July 2011

Published by:

Intelligent Transportation Systems Institute
Center for Transportation Studies
University of Minnesota
200 Transportation and Safety Building
511 Washington Avenue SE
Minneapolis, Minnesota 55455

Acknowledgments

The authors wish to acknowledge those who made this research possible. The study was funded by the Intelligent Transportation Systems (ITS) Institute, a program of the University of Minnesota's Center for Transportation Studies (CTS). Financial support was provided by the United States Department of Transportation's Research and Innovative Technologies Administration (RITA).

Table of Contents

List of Tables

List of Figures

Executive Summary

Roadway congestion in all urban areas is increasing rapidly and is causing large delays and associated costs. Bus Rapid Transit (BRT) systems are one of the more popular solutions to congestion mitigation in metropolitan areas. Optimally, BRT systems should use dedicated bus lanes to improve passenger throughput. By using narrow lanes or road shoulders, less right-of-way is required, thus facilitating the wider deployment of such "busways". The narrow lanes however cause the bus driver added stress. The use of lane assistance systems can reduce the stress level experienced by drivers and allow for better lane keeping in narrow bus-dedicated lanes. The Intelligent Vehicles (IV) Lab at the University of Minnesota has developed such a system for this purpose.

The IV Lab lane assist system uses dual frequency differential GPS (DGPS) for high accuracy position information. This position information is used in conjunction with a geospatial database containing the road geometry and lane boundary positions required for a lane assistance system. In urban environments, where tall buildings, overpasses, and other obstructions to the sky are present, DGPS suffers from inaccuracies and outages. The work herein proposes a method for replacing DGPS sensing with a high accuracy vehicle positioning system which fuses data from RFID (Radio Frequency IDentification) and LiDAR (Light Detection and Ranging) curb detection.

A Vehicle Positioning System (VPS) was originally developed by the IV Lab to provide lane level, "which lane on the road," position of a vehicle with respect to a known reference (i.e. a mile marker or start of roadway) by the use of encoded position information in RFID tags on the roadway, read by the vehicle. The lateral position resolution of VPS is constrained to one lane width, which is insufficient for lane assistant systems. Thus, in-lane level ("where in the lane") lateral position estimation was supplemented by a LiDAR unit that generates an accurate position of the vehicle with respect to the curb, which is cross referenced with a map database that provides the distance from the lane center to the curb, thus providing the vehicle's lateral offset from the lane center. On-board odometry is used to maintain accurate longitudinal position in between tag reads. By fusing the information from the VPS, LiDAR, and on-board odometry, high accuracy, "where in lane" level vehicle positioning can be maintained from this enhanced VPS during DGPS outages.

The enhanced VPS enabled IV Lab lane assist system was outfitted on the IV Lab research bus. The lane assistance system is characterized based on three characteristics.

1. lateral position accuracy
2. ride quality
3. automated lane keeping

The vehicle's lateral offset estimates from the enhanced VPS were compared to estimates post-processed from high accuracy DGPS position data. The data from both trials show that the mean difference between the lateral offset found by the enhanced VPS and that found by DGPS is under 0.4 cm with a standard deviation under of 4.6 cm.

The ride quality of the research bus was characterized when automated lane-keeping was operating using enhanced VPS, compared to GPS as well as when manually operated. The ride quality was quantified by measuring lateral acceleration from an inertial measurement sensor. The differences between the mean lateral acceleration for the VPS enabled system and the other modes of operation were under three thousandths of a G and the standard deviation differed by less than seven thousandths of a G, proving the ride quality between the modes of operation are virtually indistinguishable.

The haptic feedback through the steering wheel provides a level of automated lane keeping to the bus when the lane assist system is operating. The feedback is controlled by a PID steering controller within the lane assist system, which drives a servo motor connected to the steering wheel. The performance of the lane-keeping offers some insight into how the lane assistance system performs. Lateral offset data was collected during enhanced VPS enabled lane assistance operation of the bus to quantify the performance of the automated lane-keeping. 2,099 data points were collected over two trial runs on the university transitway from Minneapolis to St. Paul. The IV Lab research bus is 2.59 meters wide and operates in lanes as narrow as 3.05 meters. This leaves 0.23 meters on each side of the vehicle. Although the data shows that the lane boundary limits are at most 1 ½ standard deviations from the means described in Figure 36 and Figure 37, the lane boundaries are still crossed at times. This is assumed to happen not from the position errors in the enhanced VPS, but from sub-optimal steering controller performance. Increased performance can be obtained from automated lane-keeping by optimizing the steering controller.

Overall, the implementation of the VPS enabled IV Lab Lane Assistance System was shown to be successful since the in-lane (where in the lane) level position accuracy was within the required level, the ride quality was indistinguishable from DGPS and manual operation, and the lane-keeping performance was adequate.

Further improvements to the enhanced VPS can be made to increase the likelihood of large scale deployment on BRT systems. Procuring an RFID reader with a higher read frequency will increase the accuracy of the VPS updates by an order of magnitude (1.0 to 0.1 meter error at 50 mph). Optimizing the steering controller in the enhanced VPS enabled IV Lab lane assist system will allow for increased performance of automated lane-keeping and haptic feedback.

Further research could also be directed at increasing the accuracy and robustness of the LiDAR curb detector. The probability of false detections could be attenuated by more effective LiDAR data filtering. If data points that are not part of the curb can be predetermined and removed, the algorithm can be more robust and efficient. Also, it was assumed that vehicle roll had no effect of lateral position measurements from the LiDAR. This assumption has minimal effects if the vehicle roll angle is repeatable for a given location on the road, but if potholes or other exogenous factors induce vehicle roll angle, lateral position measurement errors could be significant. An IMU could be used to measure the vehicle roll induced by bumps, ruts, etc, and mitigate the lateral position errors due to this type of noise.

Perhaps the biggest hurdle that stands in the way of large scale deployment of the enhanced VPS is the requirement that the vehicle needs a clear view of a curb or other easily recognizable three dimensional reference structure, such as a guard rail or Jersey barrier. Currently, if anything

blocks the line of sight of the curb (snow drifts, parked cars, etc.) or the vehicle is in an intersection or driveway, the enhanced VPS is inoperable. One possible solution may be to measure lateral position off of a building, light pole, etc. with a LiDAR unit when available, and then updating the vehicle's position with a two dimensional speed sensor for higher frequency estimates or when a reference structure is not available. One major advantage to this configuration is that the LiDAR sensor can be moved high enough to "look" over cars, people, and other obstacles in order to measure a lateral distance from a tall[1] structural reference, such as a building or light pole. This configuration would be less susceptible to obstacles interfering with the view of the structural reference. If a system like this were developed, it would make enhanced VPS a much more flexible and attractive system. Enhanced VPS could also be used in other applications, such as precision docking. The LiDAR curb detection algorithm can provide the lateral position accuracy needed for such an application.

[1] Meaning tall relative to a person, car, snow bank or other common obstruction

1. Introduction

A. Motivation

Roadway congestion in all urban areas is increasing rapidly and is causing large delays and associated costs. The 2007 Urban Mobility Report [1] estimated that the total costs associated with traffic congestion rose from $15 billion to $78 billion from 1982 to 2005, tabulated from 487 urban areas in the United States. The same report estimates that public transportation saved 541 million hours of delay, 340 million gallons of fuel, and $10.2 billion dollars in 2005. Many metropolitan areas are adopting BRT (Bus Rapid Transit) systems to increase ridership and further reduce traffic congestion.

Optimally, BRT systems use dedicated bus lanes to improve passenger throughput. By using narrow lanes or road shoulders, less right-of-way is required, thus facilitating the wider deployment of such "busways". The narrow lanes however cause the bus driver added stress. The use of lane assistance systems can reduce the stress level experienced by drivers and allow for better lane keeping in narrower lanes. The Intelligent Vehicles (IV) Lab at the University of Minnesota has developed such a system for this purpose, as described in [2].

The IV Lab lane assistance system uses dual frequency carrier phase differential GPS (DGPS) for high accuracy position information. This position information is used in conjunction with a high accuracy geospatial database[2] containing the road geometry and lane boundary positions required for a lane assistance system. However, there are many sources of errors affecting GPS accuracy [3]. These are:

1. Atmospheric affects: A phase shift in the signal from the GPS satellites occurs when the signal passes through the charged particles of the ionosphere and the water vapor in the troposphere.
2. Multipath: Signals from the GPS satellites may bounce off adjacent structures before reaching the GPS receiver, increasing the path distance, and thus shifting the position solution.
3. Satellite ephemeris: There are errors in the position of the satellites which contribute to positioning errors.
4. Geometric dilution of precision: The geometry of the satellite constellation can be such that the satellite sightlines can be close to collinear providing a sub-optimal position solution.

Although correction signals can compensate for atmospheric effects and satellite ephemeris, high accuracy DGPS is not always available. In urban environments, where tall buildings, overpasses, and other obstructions to the sky are present, GPS satellite signals are blocked, causing severe GPS inaccuracies and outages. The work herein proposes a method for replacing DGPS with an enhanced VPS (Vehicle Positioning System) for the IV Lab lane assist system, as described in [5] to circumvent the vulnerabilities of DGPS in urban environments.

[2] The spatial data in the geospaital database is on the order of centimeters

B. Background Information

i. VPS Overview

VPS was previously developed by the IV Lab to provide lane level (which lane on the road) position of a vehicle with respect to a known reference (i.e. a mile marker or start of roadway) as described in [4]. To achieve this, passive RFID tags are placed on the lane boundaries of the roadway[3]. The tags are encoded with a road identifier, lane boundary ID, cardinal direction of travel, and a longitudinal distance from a known reference (i.e. I-94, lane boundary 1, W, 1.1 miles from mile marker 0). As the vehicle travels down the road, it reads the tags and updates its lane-level position. The vehicle's position is determined based on which antenna reads a given tag. An illustration of a typical setup is shown in Figure 1 below.

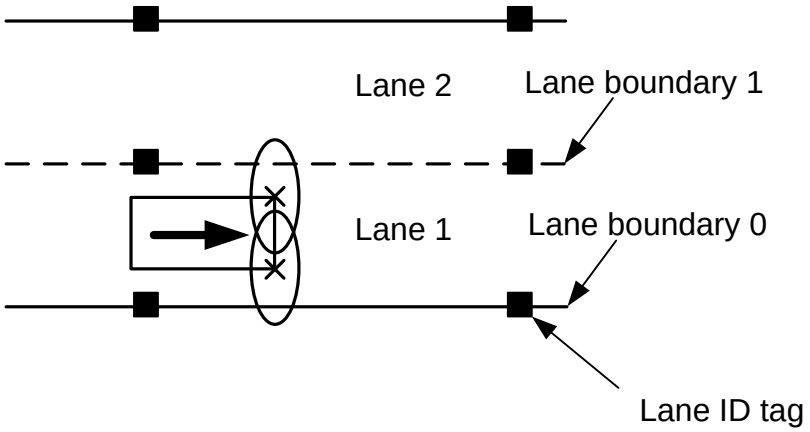

Figure 1. Illustration of typical VPS setup

The vehicle in Figure 1 can be placed in lane 1 because the left side antenna reads lane boundary 1 and the right side reads lane boundary 0.

The lateral position resolution of VPS is constrained to one lane width, which is insufficient for lane assistant systems. Thus, in-lane level (where in the lane) lateral position is supplemented by a LiDAR (Light Detection And Ranging) unit that generates an accurate position of the vehicle with respect to the curb, which is cross referenced with a map database providing lateral offset from the lane center. On-board non-contact odometry is used to maintain accurate longitudinal position in between tag reads. By fusing the information from the VPS, LiDAR, and non-contact odometry, high accuracy lateral vehicle positioning can be maintained from the enhanced VPS during DGPS outages.

ii. IV Lab Lane Assist System Introduction

The IV Lab lane assist system provides lane keeping and collision avoidance assistance to the driver to reduce the stress of operating a vehicle in a narrow lane with a tight clearance. The lane keeping information is derived from a high accuracy position measurement of the vehicle

[3] Other VPS configurations are possible as described in [4]

(obtained by the enhanced VPS[4] or DGPS) and a database containing information including the road geometry and lane boundary positions. The collision avoidance information is derived from a sensor set that includes LiDAR and radar units, which detect other vehicles, pedestrians, and other obstacles that pose a collision threat to the vehicle. This information is fed back to the driver via a quad-mode Human-Machine Interface (HMI) [2], as seen in Figure 2 below. These four modes are:

1. Graphical Head-UP Display (HUD): provides a representation of the lane boundaries and obstacles that are virtually overlaid onto the road.
2. Virtual mirror: shows a plan view of the vehicle along with LiDAR and radar targets spatially placed with respect to the vehicle.
3. Haptic feedback through a torque actuated steering wheel: in the event that the vehicle drifts in the lane, the actuator will guide the steering wheel to center the vehicle. Note that the torque applied to the steering wheel is such that it can be easily overcome by the driver if desired.
4. Tactile feedback through vibration in the seat: if the vehicle drifts near the left lane boundary, the left side of the seat will vibrate and vice versa.

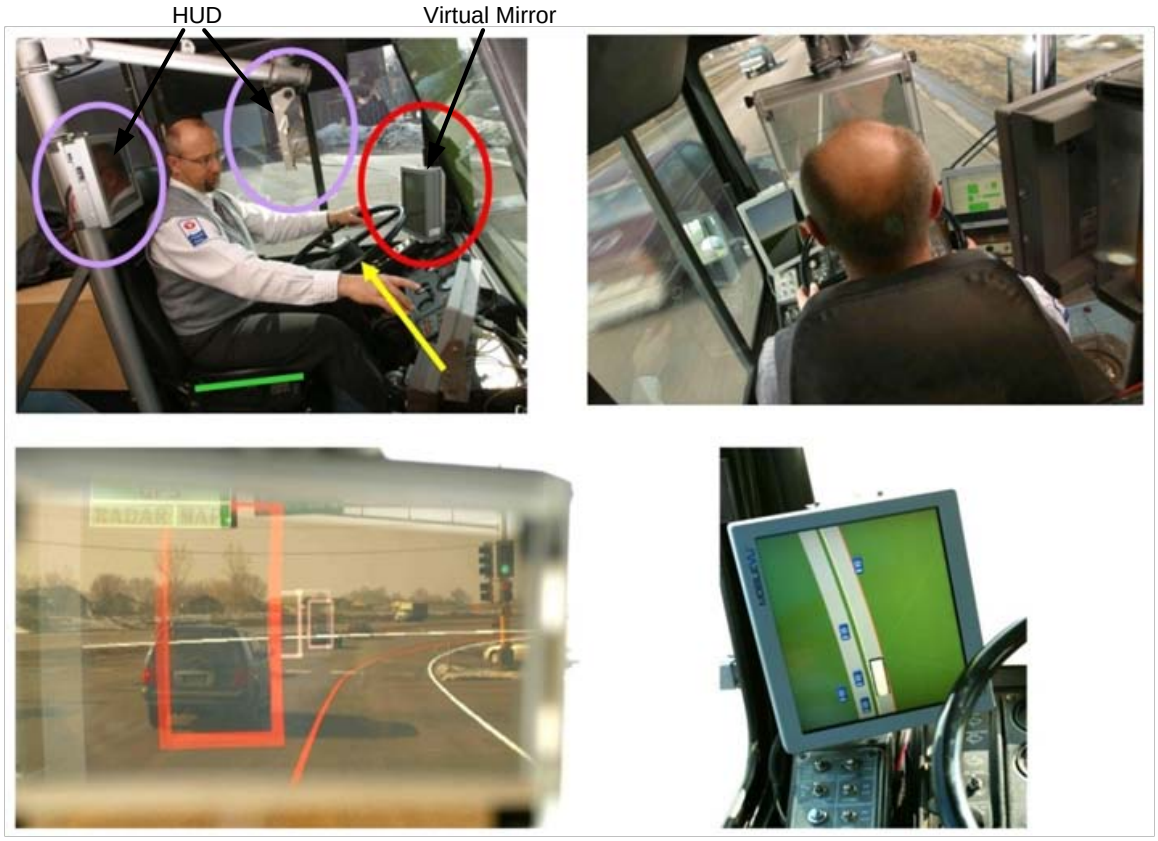

Figure 2. Lane assistance feedback via HMI

[4] Enhanced VPS in this document refers to VPS augmented with odometry and LiDAR curb detection

The upper left picture in Figure 2 shows all of the components of the HMI. The lower left picture shows the view through the HUD, and the lower right picture shows the virtual mirror. The driver has the option of disabling any of these modes of feedback to ensure comfort during operation.

C. Previous Work

There have been many positioning systems developed in the past 15 years for vehicles. The University of California at Berkeley developed a system based on magnetic sensing as described in [6,18]. This system provides high accurate position information, but does not located the vehicle unambiguously on the roadway at each magnet measurement, which means that the position information is relative to the last magnet observed and not to any fixed coordinate frame. Although, a binary message (that can offer a road ID, lane ID, road curvature, etc) can be formed by choosing the polarity of a series of magnets as described in [18], a large number of magnets must be used to get any useful information. The RFID tags used in testing the VPS system have a capability of providing a 96 bit message. For the magnetic guidance system to provide an equivalent message, 96 magnets must be read. These magnets are typically 1.2 meters apart, thus to receive a 96 bit message from the magnets would require the vehicle to travel 115 meters. This can take a significant amount of time, especially for a lane assistance system. The magnetic guidance system is also expensive, $10,000 per lane mile as documented in [18], and labor intensive to install compared to the VPS enabled lane assistance system. Many vision based driver assistance systems, such as RALPH [7], have also been developed. However, vision based systems are susceptible to varying lighting conditions due to changes in weather and are non-functional when the quality of the lane striping is poor or is covered by snow.

Using a fusion of RFID based positioning, LiDAR curb detection, and odometry is a novel concept for providing “where in lane” level position information. However, curb detection and odometry independently have previously been investigated thoroughly. There are systems that use computer vision and LiDAR to detect curbs [8,9], and systems that use 3D LiDAR and vision [10]. There is also a system that uses a “laser light striper” and computer vision to detect curbs [11]. These systems are designed to detect square curbs on flat roads. The curb detecting system presented in this work detects regular curb shapes as well as jersey barriers, guard rails, or any other fixed three-dimensional reference structure that is adjacent to the road and has a consistent shape. The system is fully functional without using computer vision.

Other RFID based positioning systems for vehicles have also been developed [12-15]. All of the work found relating to RFID vehicle positioning only gives the vehicle position updates when a new RFID tag is read, and there are no supplemental sensors to improve vehicle position estimates. Furthermore, this location estimate is only as accurate as the read range of the RFID reader. VPS fused with a high accuracy lateral position estimate can provide a more precise vehicle location that can be used in a lane assistance system, whereas previous RFID positioning systems cannot.

D. Document Overview

The following chapters describe the fusion of VPS, odometry, and LiDAR curb detection in the Intelligent Vehicles Lab’s lane assist system. In chapter two, the enhanced VPS concept (fusion

of VPS augmented with odometry, and LiDAR curb detection) is explained in detail. In chapter three, the main components of the enhanced VPS are characterized. The required longitudinal accuracy of VPS is derived based on the required lateral accuracy needed by a lane assistance system. The attainable longitudinal accuracy of VPS augmented with odometry is then derived based on the specific hardware used in the prototype system and the road geometry of the proving grounds. Also, the accuracy and reliability of the LiDAR curb detector is quantified. In chapter four, the implementation of the IV Lab lane assistance system using the enhanced VPS is described and characterized. The performance of the system is analyzed based on the quality of the lateral position accuracy provided by the enhanced VPS, the ride quality under automated lane-keeping, and the performance of the automated lane-keeping quantified by the lateral lane center to vehicle centerline offsets. The final chapter offers conclusions on this work and recommendations for future research.

2. Enhanced VPS

A. System Overview

The IV Lab lane assist system provides lane keeping and collision avoidance assistance to the driver of the vehicle to reduce stress while operating in a narrow lane or road shoulder. In order to provide lane keeping feedback, the system must determine the instantaneous position of the vehicle with respect to the center of the lane within which it is operating. The approach taken by this work is to use VPS in conjunction with on-board odometry and LiDAR curb detection to determine a vehicle's instantaneous position on the road, and a map database to store road features including lane center position with respect to the curb, curb shapes, and the desired steering angle for the present road curvature. If the vehicle's position with respect to the curb is known and the lane center position with respect to the curb is known, then the lateral offset can be determined by the difference in the two positions as seen in Figure 3.

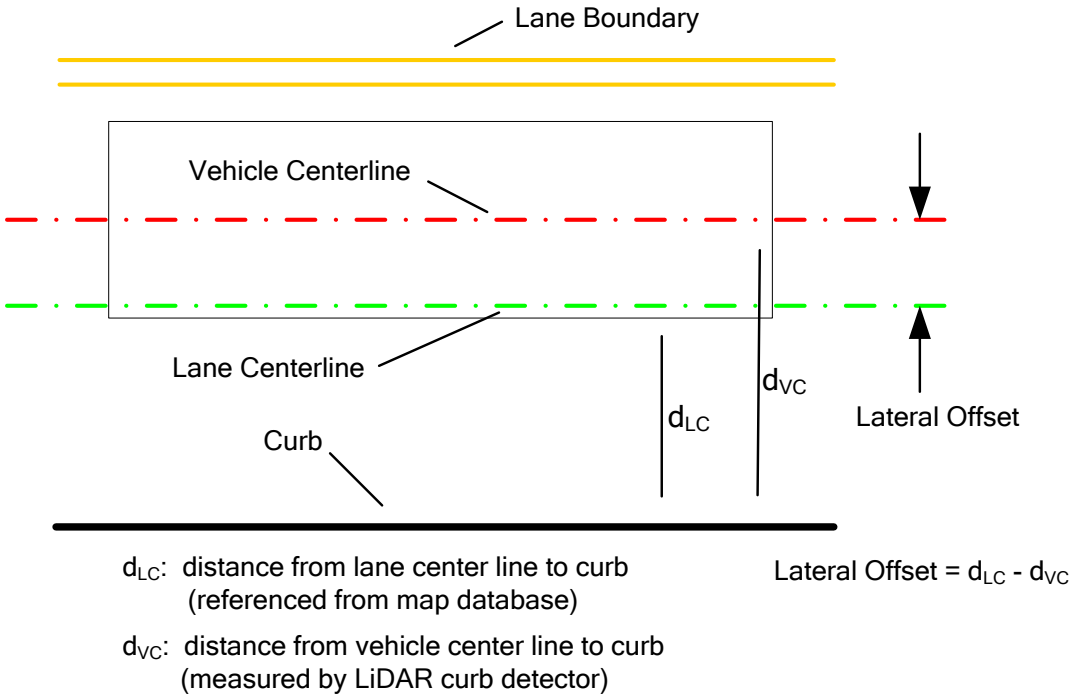

Figure 3. Illustration of lane offset

The vehicle centerline position with respect to the curb is found by the LiDAR curb detector. This requires the vehicle to have a clear view of the curb[5]. The lane centerline position with respect to the curb is extracted from the map database based on the longitudinal position of the vehicle down the lane, which is provided by VPS augmented with odometry.

Desired steering angle information stored in the map database is used as a feed-forward term in the controller driving the haptic feedback provided by the steering wheel. This feed-forward

[5] Solutions to this limitation are discussed in chapter five section E

term increases the stability of the controller by providing a priori knowledge of the desired steering angle needed to negotiate the given road curvature. The following sections describe how VPS determines vehicle position and how this information is supplemented by odometry and a curb detection sensor to get the high accuracy "where in lane" level position information needed for the lane assistance system.

B. VPS

i. RFID Technology Overview

RFID systems allow data to be wirelessly transferred from a passive transponder to an RFID reader via radio waves. An RFID system consists of three major components:

1. RFID tags (transponders) encoded with data (typically 96-128 bits)
2. RFID reader
3. RFID TX/RX antenna set

Data is transferred from the tag when the TX and RX antennas are in close proximity to the tag. The TX antenna transmits enough electro-magnetic energy to the tag for it to send a radio signal back with the encoded data. This radio signal is pickup up on the RX antenna and decoded by the RFID reader to extract the data into a usable form. This communication sequence is depicted in Figure 4 [16].

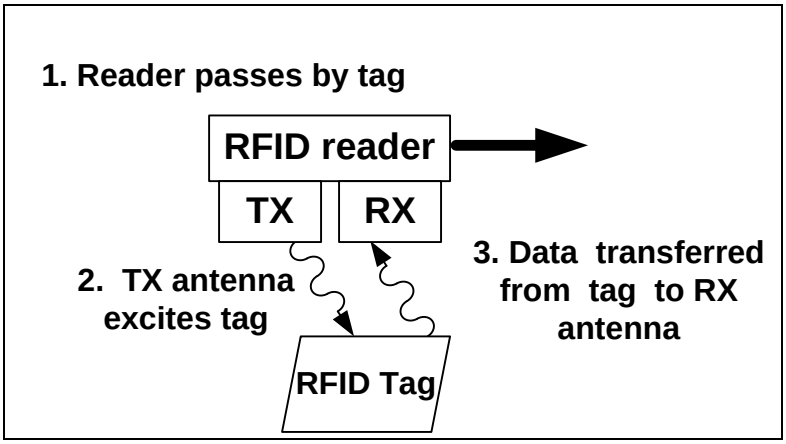

Figure 4. Data transfer sequence

ii. Lane Level Positioning Using VPS

To perform lane level positioning, RFID tags are placed on each side of the vehicle in the lane boundaries of the roadway[6], each encoded with a unique ID. As a vehicle passes by the RFID tags, the RFID reader acquires the tag information using a TX/RX antenna pair on each side of the vehicle. The tag ID is either referenced in a database for, or encoded with, a road identifier, lane boundary ID, and longitudinal path distance from a known reference.[7] Lane position can be

[6] Other VPS configurations are possible as described in [4]
[7] The longitudinal axis is parallel to the centerline of the lane

derived based on which antenna pair reads the specific lane ID tag and the encoded information in the tag.

Figure 5 illustrates a typical VPS configuration. In this example, the vehicle at position 1 would be placed in the right lane because the left antenna set reads a tag on the middle lane boundary and the right antenna set reads a tag on the right most lane boundary. During a lane change maneuver, both antenna sets read a tag on the same lane boundary, indicating that the vehicle is straddling a lane. The tags also reference what road the vehicle is on, the direction of travel, and longitudinal position down the road in which the tag is placed. The longitudinal spacing of the tags depends on the application. For instance, a collision avoidance system would require higher accuracy longitudinal position information than a tolling application.

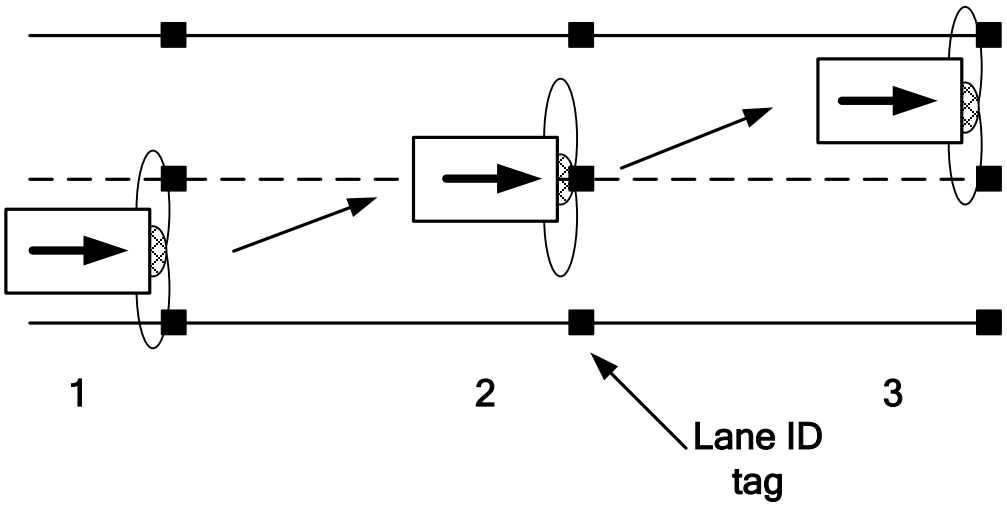

Figure 5. RFID tags are located in the lane boundaries and two antenna sets are located on each side of the vehicle

C. Augmenting VPS with Odometry and Lateral Position Information

i. On-board Non-contact Odometry

VPS does not provide sufficient longitudinal position resolution for a lane assistance system. Thus, odometry is used to augment VPS longitudinal measurements. Odometry provides longitudinal position estimates from the last VPS position measurement at the higher frequencies needed to maintain sufficient position measurement resolution. Odometry is achieved by integrating the speed of the vehicle, obtained in this project by a non-contact Doppler-based speed sensor as described in [5].

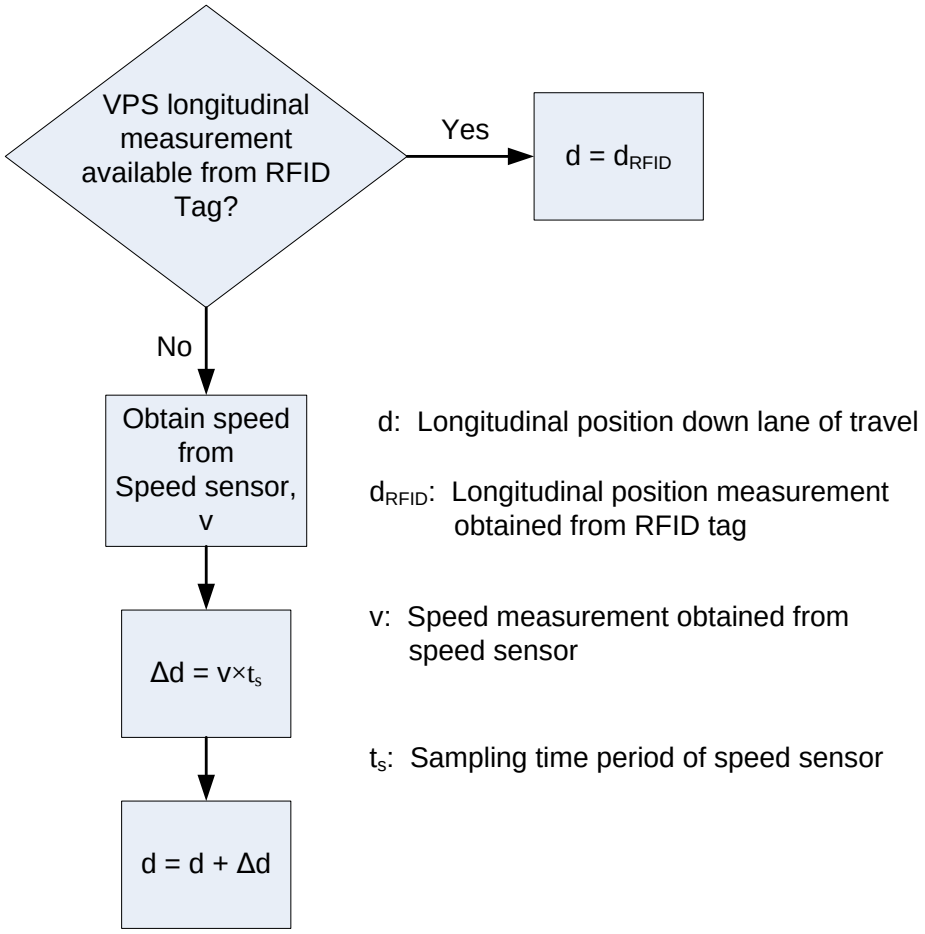

Figure 6. Flowchart of the odometry process

It is important to note that the accuracy of the speed sensor determines the amount of drift, or increasing amounts of error, in the odometry estimate. These drift characteristics determine the spacing of the VPS longitudinal position measurements needed to maintain the required longitudinal position accuracy for the lane assist system. The VPS measurement spacing is derived in chapter three, along with a more detailed explanation of how the odometry process is carried out.

ii. Lateral Positioning

VPS provides only lane level positioning (what lane the vehicle is in), and does not provide the in-lane level positioning (x centimeters from lane center) capability required by a lane assistance system. To achieve high accuracy lateral positioning, a LiDAR sensor is used in a curb detection system to give a measurement of the distance between the vehicle and the curb. If the lane center position is known with respect to the curb, and the vehicle distance to the curb is known, the lateral offset between the vehicle and the center of the lane can readily be determined, as previously shown in Figure 3.

The LiDAR unit used in this implementation of a curb detector is the Sick LMS 220. This unit has the ability to produce 100^o field-of-view scans with $1/4^o$ resolution at 33 Hz and has a range

up to 30 meters. The LiDAR is mounted such that it scans in a plane perpendicular to the curb face, as shown in Figure 7.

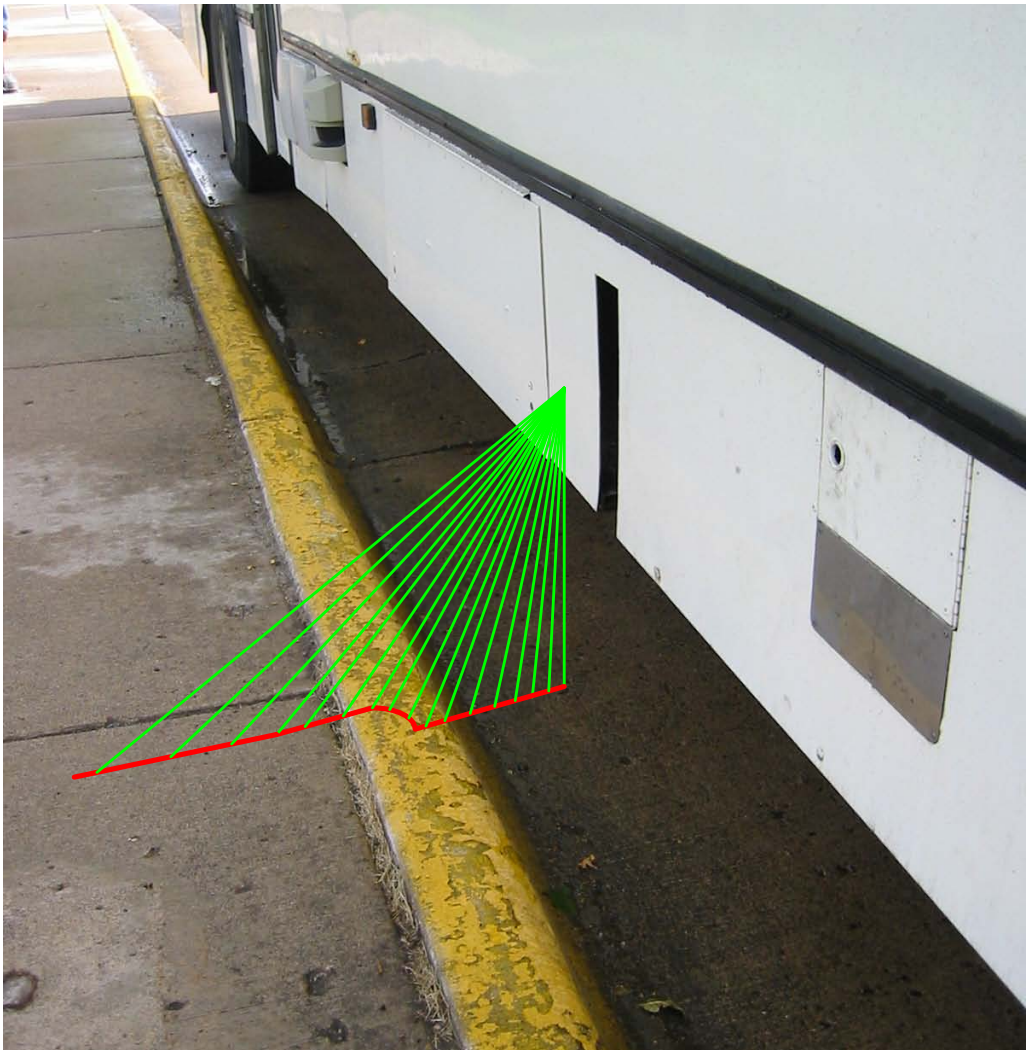

Figure 7. LiDAR unit mounted vertically on vehicle providing a cross section scan of the curb

The curb detection algorithm sweeps a curb model, which is stored in the map database, over each data point in the LiDAR scan set. The curb detection algorithm determines the location where the curb shape correlates best with the LiDAR scan data points[8], S_1 through S_N. The spatial resolution of the LiDAR data deteriorates as the distance between the curb and LiDAR sensor increases, thus the algorithm ignores LiDAR data that is five meters or more from the sensor. This threshold value of five meters was chosen based on the characterization (described in chapter 3) of the curb detector and the specific LiDAR sensor used in the experiments. A detailed explanation of the curb detection algorithm is located in Appendix A on page 64. If the LiDAR data doesn't meet the correlation thresholds, the curb detection algorithm reports that no

[8] As seen in Figure 8 when curb model is overlaid onto data point S_B

curb was found in the data and the system is disabled until a curb is detected. The correlation threshold was calibrated during testing by a trial and error method. The LiDAR unit is fixed to the bus, allowing the curb position to be determined with respect to the vehicle with a polar to Cartesian coordinate transformation (the roll angle of the bus is ignored in the calculation of curb position). The position of the vehicle with respect to the curb is then compared with the distance from the lane center to the curb (acquired from the map database based on the information from VPS and odometry) to determine the vehicle's lateral offset from the lane, thus providing "where in lane" level vehicle position.

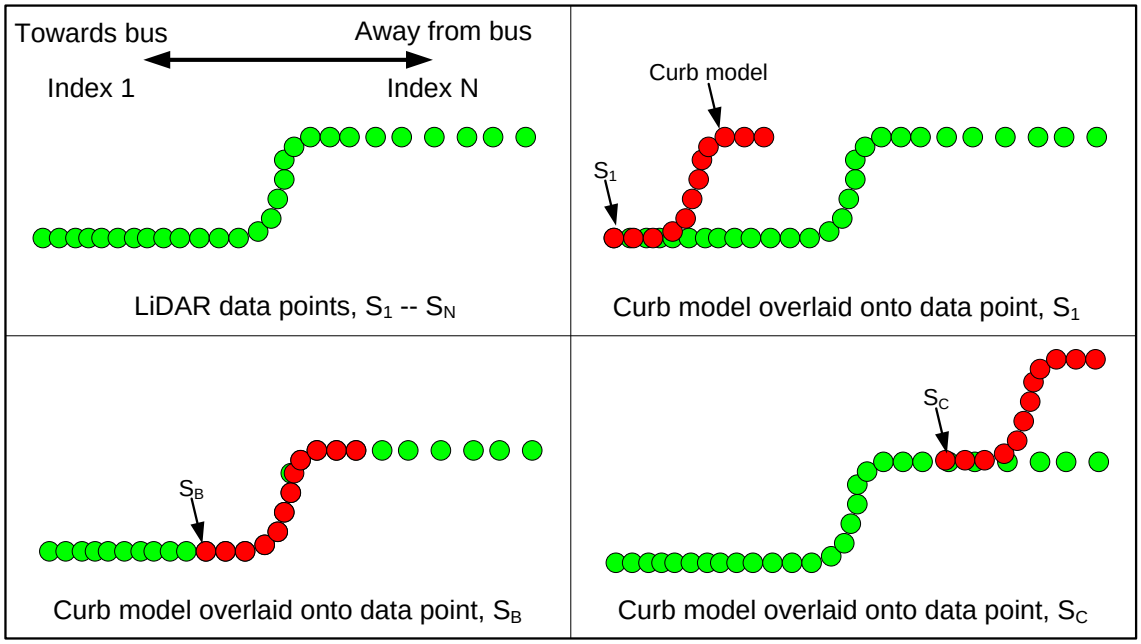

Figure 8. Curb model overlaid on LiDAR data points where data point index C > B > 1 (note that not every scan point is shown to be overlaid with the curb model)

D. Map Database and Vehicle Position Determination

i. Map Database Structure

The map database stores geometric information about the roadway, which is necessary to compute the vehicle's position within the lane. The database has three different types of tables: curb model tables, RFID tables, and road segment information tables. The curb model tables store the curb model shapes that are used in the curb detection algorithm. There is a unique curb model table for every unique curb shape that exists on the roadway. The RFID table stores the information that the RFID tags reference (i.e. unique RFID tag ID, road identifier, lane identifier, longitudinal distance). The segment information table stores the geometric information about the lanes on the roadway. There is a unique segment information table for each lane. The following is a database model of the map database:

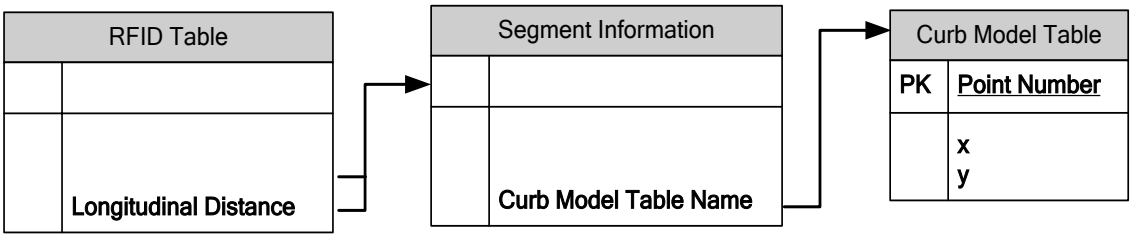

Figure 9. Database model

Table 1. Description of database fields

Database Field Name	**Description**
Tag ID	Unique RFID tag ID used as a primary key to query RFID table information
Road ID	Unique ID used to reference a road on the VPS network
Lane ID	Unique ID referencing a specific lane on the road
Longitudinal distance	Path distance down the roadway from a common reference point (meters)
Lane center position	Distance from the curb to the center of the lane (meters)
FF steering angle	Desired steering angle at the given longitudinal distance. Used as a feed-forward term in the steering wheel controller (radians)
Curb model table name	The unique name of the curb model table to query for curb model shape information
Point number	Unique point ID used as a primary key to index model points
x	Given x component of the model point position with respect to the position of the first point in the curb model shape (meters)
y	Given y component of the model point position with respect to the position of the first point in the curb model shape (meters)

The RFID table is queried, based on the tag ID (primary key[9]), for the road ID, lane ID, and longitudinal distance every time an RFID tag is read. The lane ID and the longitudinal distance, which is updated by odometry in between tag reads, is used to query lane center position, feed-forward steering angle, and the curb model table from the segment information table. The

[9] The primary key is a unique index used for optimally querying the given SQL database table

specific curb model table obtained from the segment information table is then queried for the curb model shape required for curb detection. However, for efficiency, the curb model table is only queried when there is a change in curb model tables.

ii. Determining the Vehicle's Lateral Position

In order for VPS to initialize, at least one RFID tag must be read. Once this occurs, the RFID table is queried and lane level position is obtained (i.e. I-94 Westbound, Lane 1, 100.5 meters from mile marker 1). This information is used to query the segment information table for the lane center position and feed forward steering angle. With the information from the curb detector, the lateral offset (difference in position of the vehicle center line and lane centerline) can be determined. A process flowchart summarizing the sequence of events in the data processing loop is shown in Figure 10.

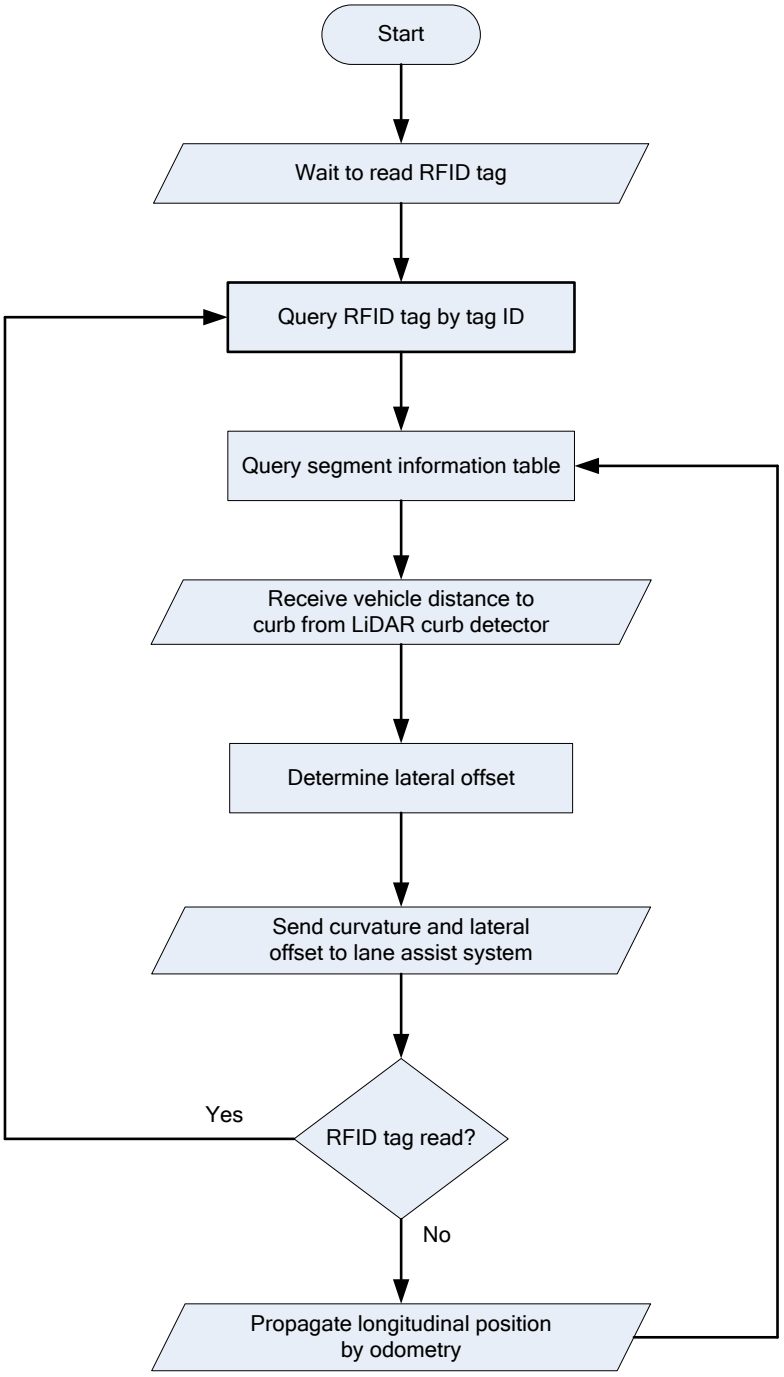

Figure 10. Data processing loop for lane offset determination

The lateral offset and steering angle information is then passed into the steering controller, associated with the haptic feedback, the HUD lane warning system, and the seat vibration controller.

iii. Building the Map Database

The map database is built with raw data collected from the RFID reader and tags, speed sensor, LiDAR curb detection system, and steering wheel motor optical encoders. Certain assumptions must be made to insure that the map database is accurate enough for the lane assistance system:

- When collecting the raw data from each of the sensors, the vehicle centerline is in-line with the lane centerline during manually driven operation
- The steering angle measured is the correct steering angle for the given road curvature
- Uneven or bumpy roads and road curvature, which may induce vehicle roll and pitch, will be repeatable and not cause a reduction in the accuracy of the position estimates derived from map database information

1. Building the Curb Model Table

The curb model table holds the geometry information of the curb model shape used in the curb detection algorithm. Curb model tables are created by collecting LiDAR data for each curb shape. The section of data that contains the curb shape is extracted and averaged to reduce the noise from the LiDAR measurements. The data is converted into Cartesian coordinates, and the origin of the coordinate frame is moved from the sensor origin to the first data point in the curb model. This transformation allows the data to be conveniently used in the correlation algorithm of the curb detector. The index and (x, y) positions of the data points are then inserted into a curb model table associated with the curb shape.

2. Building the RFID Table

The RFID table holds the longitudinal position information referenced by the RFID tag identification numbers. The spacing of the tags on the roadway is chosen based on the characteristics of the RFID reader, non-contact speed sensor, and road geometry. This is explained in further detail in chapter three. The longitudinal positions of the tags are determined with respect to a reference point, which is chosen to be one of the tags on an endpoint of a lane on the roadway, as seen in Figure 11. The longitudinal spacing of the tags is found by the same method of odometry (as well as the same speed sensor and RFID hardware) that is used in the enhanced VPS system. These longitudinal positions are inserted into the RFID table along with the road and lane they are placed in.

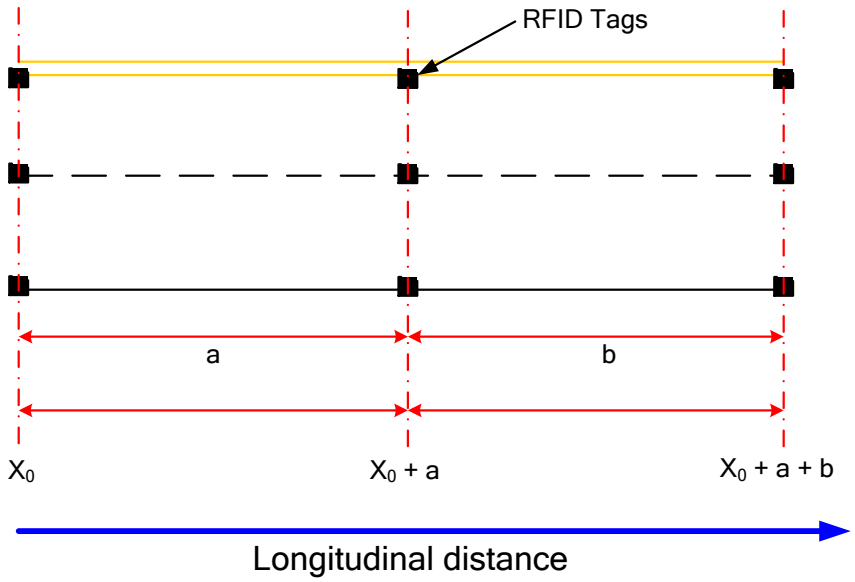

Figure 11. Illustration of RFID longitudinal distance with respect to reference point X0 (a does not have to equal b)

3. Building the Segment Information Table

The segment information table has lane center position, feed-forward steering angle, and a curb model table reference with respect to the longitudinal distance down the lane. The segment, or lane, information is surveyed by the vehicle performing a "mapping run" where the vehicle drives down the center of the lane at all times. Lane center position is surveyed using the VPS augmented with odometry and the LiDAR curb detection system to create the distance from the vehicle to the curb as a function of longitudinal distance from a known reference point. The desired steering angle is also measured as a function of longitudinal distance from a known reference point. The desired steering angle is a measure of the steering motor position. The steering motor position is measured with an absolute optical encoder.

Changes in curb shapes are also surveyed with respect to the longitudinal distance supplied by VPS and odometry, and the respected curb model table names are inserted into the segment information table.

3. Characterization of Sensors

A. VPS Augmented with Odometry

i. Introduction

The VPS augmented with odometry must provide accurate longitudinal position estimates to ensure that the correct road geometry is queried from the map database. In order to quantify the required accuracy needed, it is necessary to characterize the geometrical properties of the roadway being driven. For instance, if the road is straight and the distance from the curb to the centerline of the lane is constant, longitudinal position is irrelevant. However, if the road has curves and the distance from the curb to the centerline of the lane varies, then an accurate measure of longitudinal position is necessary so that accurate feedback can be provided to the vehicle's operator.

There are primarily two factors that can cause significant lateral position errors from erroneous feedback due to longitudinal position estimation errors. These factors are:

1. Variation in lane center to curb distance
2. Curves in the road.

For example, the distance between the curb to the centerline of the lane can vary when parking lanes, protected right turn lanes, or bus stops exist.

The variables used in the following discussion are defined as:

x – Actual longitudinal position
$\hat{x}$ – Longitudinal position measurement from VPS and odometry
$\tilde{x}$ – Longitudinal position measurement error, ($\tilde{x} = x - \hat{x}$)
$\tilde{y}$ -- Lateral position error induced by erroneous feedback from lane assist system
m – Curb slope, $m = \Delta y/\Delta x$, as depicted in Figure 12 (can be thought of as the derivative of the distance from the curb to the lane center as a function of longitudinal position)
r – Radius of curvature error, (r = smallest radius of curvature of the roadway)

Figure 12 shows a situation where a variation in the distance from the lane center to the curb accounts for an error in the lateral position due to longitudinal position estimate inaccuracies. If the vehicle is located at $x = x_0$, but due to error in the longitudinal position estimate, x_E, the vehicle positioning system incorrectly locates the vehicle at $\hat{x} = x_0 + x_E$, an error in the lateral position estimate will exist. At the longitudinal position $x = x_0 + x_E$, the desired distance from the vehicle to the curb, d_{LC}, is larger than at $x = x_0$, $d_{VC.}$ This will cause the guidance system to determine that the vehicle is too close to the curb by $d_{LC} - d_{VC}$.

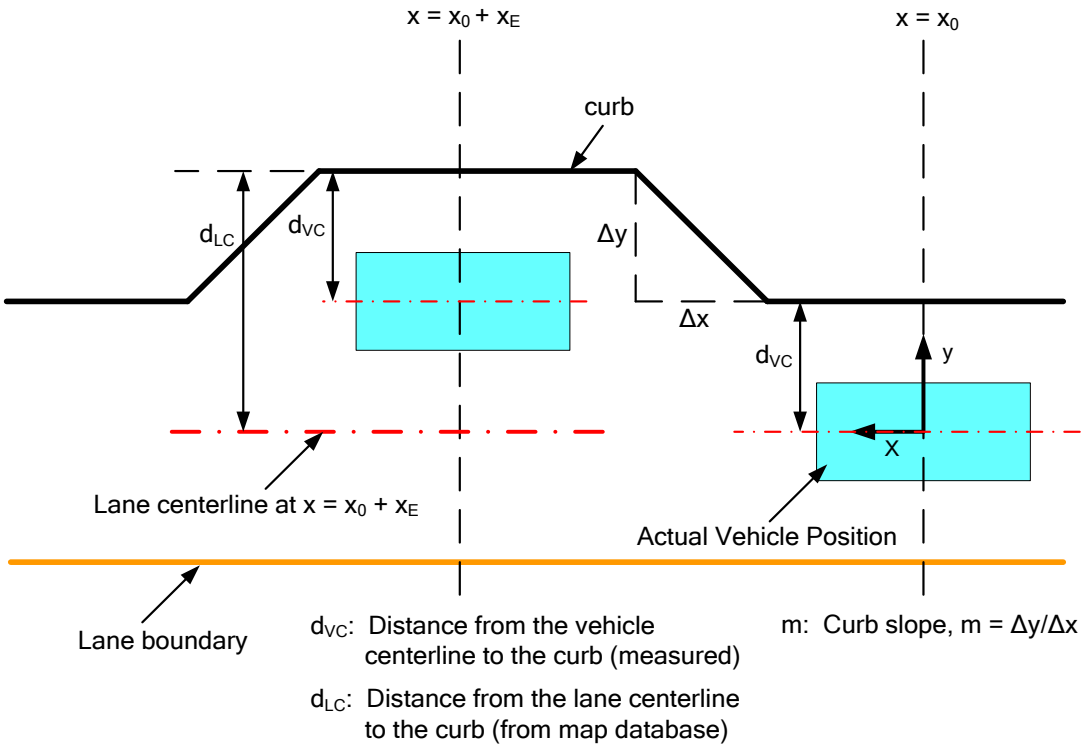

Figure 12. Longitudinal measurement error causing lateral position error due to varying lane center to curb distance (longitudinal position error is exaggerated for illustrative purposes)

Figure 13 shows a situation where an error in the longitudinal measurement causes the vehicle to enter a curve prematurely. This is due to the erroneous feed-forward steering angle information referenced from the map database at $x = x_0 + x_E$. The feed-forward steering angle at $x = x_0$ should be zero because it is in a straight segment, and the feed-forward steering angle at $x = x_0 + x_E$ should be non-zero because that location is in a curve. If the vehicle is actually at $x = x_0$, but due to longitudinal measurement errors the vehicle's position is determined to be at $x = x_0 + x_E$. The incorrect steering angle will be provided and the vehicle will enter the curve prematurely.

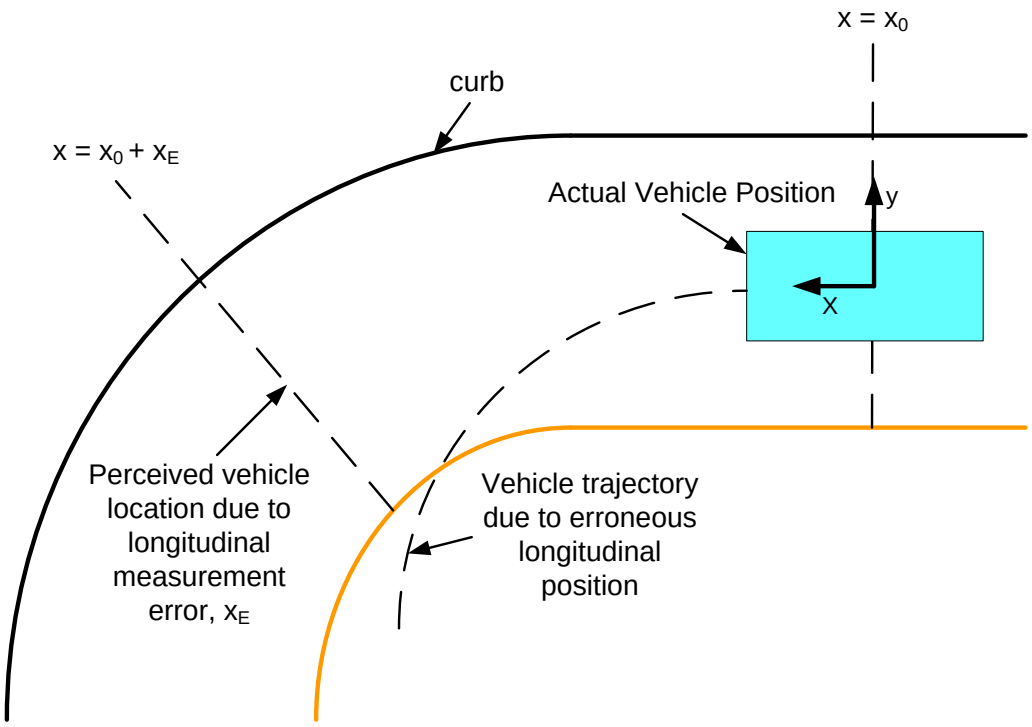

Figure 13. Longitudinal measurement error causing vehicle to turn prematurely

ii. Derivation of Required Longitudinal Accuracy

The equations relating longitudinal position errors to lateral position errors are as follows:

$\tilde{y} = m\tilde{x}$ (Eq. 1) lateral position error due to varying curb to lane centerline distance

$\tilde{y} = r - \sqrt{r^2 - \tilde{x}^2}$ (Eq. 2) lateral position error due to radius of curvature error

The derivation of equation 2 can be found in Appendix A on page 65.

Equations 1 and 2 are summed to give the total lateral position error, $\tilde{y}$, for a given longitudinal position measurement error, $\tilde{x}$,

$\tilde{y} = m\tilde{x} + r - \sqrt{r^2 - \tilde{x}^2}$ (Eq. 3)

For vehicle guidance applications the lateral position errors must be minimal. Therefore, a design specification of the maximum allowable error in lateral position was chosen to be 10 cm, which is comparable to the DGPS position errors characterized in [17]. Rearranging equation 3 into quadratic form,

$0 = \tilde{x}^2 + \frac{2m(r-\tilde{y})}{m^2+1}\tilde{x} + \frac{(\tilde{y}-2r)}{(m^2+1)}\tilde{y}$ (Eq. 4)

$\tilde{x}$ can be solved for $\tilde{y}$ = 10 cm and r = 50 meters, which is a typical radius of an interstate clover leaf, and m = 0.0852. The slope of the curb, *m*, was chosen from measuring extreme curb slopes on the university transitway, which was used as the proving grounds for this project. From these

assumed values, the maximum allowable error in a longitudinal position measurement is 1.05 meters.

iii. Attainable Longitudinal Accuracy from VPS Measurement

The vehicle's longitudinal measurement is updated by the VPS system every time the RFID reader passes an RFID tag. However, longitudinal measurement errors exist because the read frequency of the RFID reader is not infinite. The Symbol XR400 was the RFID reader procured for this work. The specifications for the XR400 are shown in Table 2.

Table 2. XR400 RFID reader specifications

Frequency	UHF band, 902-928 MHz
RF Power output	Up to 30 dBm
RFID standard	EPC Gen 2
RF connectors	Reverse TNC
Power Supply	24 VDC @ 1.2 amps
External Interfaces	USB, RS-232
Network connectivity	10/100 Base T Ethernet, RJ45
Memory	Flash 64 MB, DRAM 64 MB
Operating System	Microsoft Windows CE 4.2

The excitation signals that are needed to read the RFID tags are sent by the Symbol XR400 RFID reader approximately every 87 milliseconds[10]. As the RFID reader passes the RFID tag, the longitudinal position of the vehicle when the tag enters and exits the read field is measured and recorded (i.e. first and last tag read positions). The midpoint of these two locations is the best estimate as to where the reader passed over the tag. If the read frequency is infinite, these locations are known, but since the read frequency is finite, there is uncertainty in the accuracy of the said positions.

Figure 14 shows an example of the reader passing over a tag. The tag is shown at five different instances in time as it passes through the read field of the reader. These instances in time reflect the tag position in the read field of the reader at the time when the reader emits an excitation signal to the tag.

[10] Excitation signal characteristics for the XR400 RFID reader were experimentally determined by collecting 150 samples. The mean time between waves was 73.2 milliseconds with a 4.8 millisecond standard deviation. A period of 87 milliseconds was determined by taking a 99.9% one-sided confidence interval.

$t = t_1$: The first instance in time when the reader emits an excitation signal when the tag is within the read field. This occurs at location X_1.

$t = t_4$ The tag is in the read field for the last time when an excitation signal is sent by the reader. This occurs at location X_4. Note that due to the finite frequency at which excitation signals are sent, X_4 may not represent a tag at the outside boundary of the read field.

$t = t_5$ The tag, at X_5, is just outside the read field when the excitation signal is sent by the reader, thus the tag cannot be read.

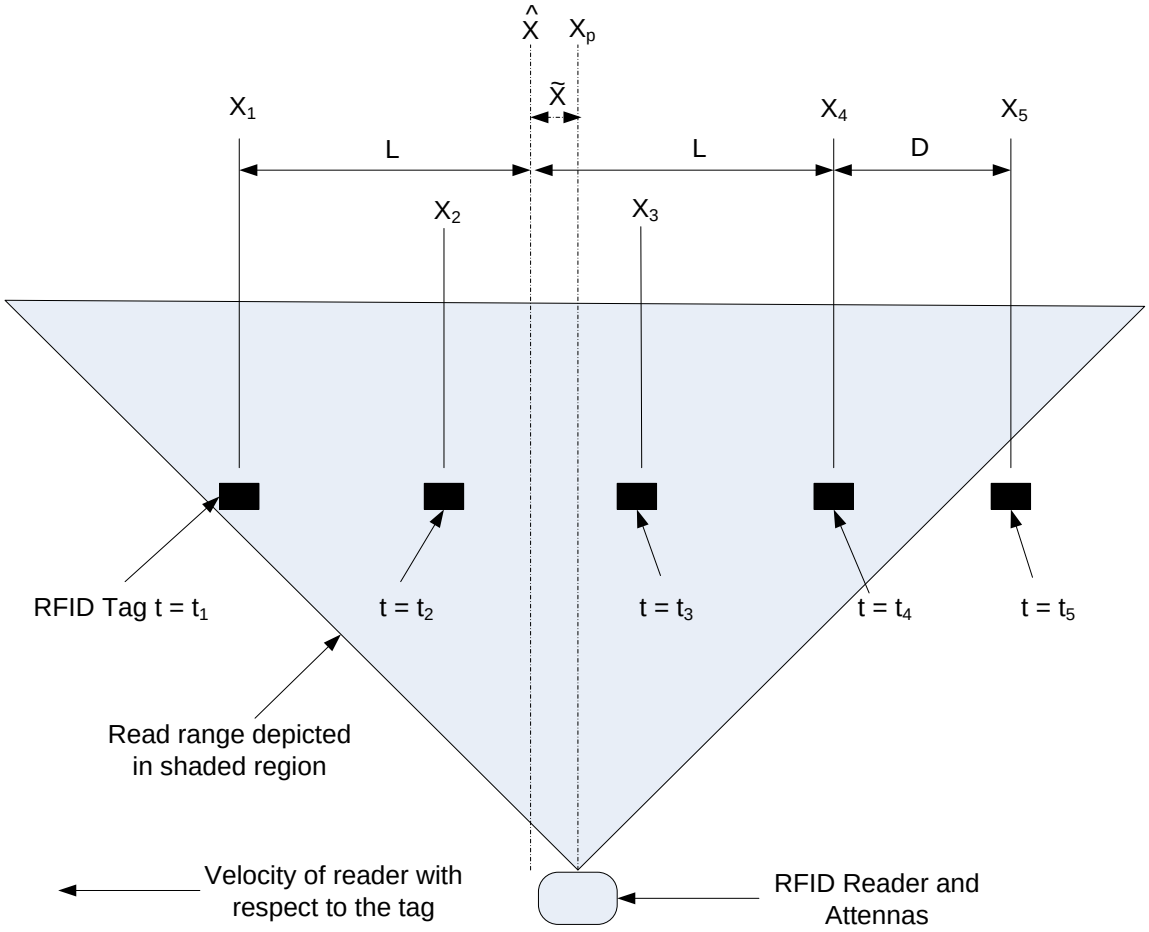

Figure 14. RFID reader (on vehicle) passing over an RFID tag at time samples t1 - t5

This example shows the maximum error, $\tilde{x}$, possible in the estimate of where the reader passes over the tag because at $t = t_4$ the last tag read is recorded at the furthest distance possible to the actual end of the read field and the first tag read is recorded at the beginning of the read field.

$$\tilde{x} = X_p - \hat{X} \qquad \text{(Eq. 5)}$$

where X_p is the location of when the reader passes over the tag, and $\tilde{x}$ is the estimate of where the reader passes over the tag.

$$\hat{X} = \frac{X_1+X_4}{2} = \frac{X_1+2L}{2} \qquad \text{(Eq. 6)}$$

$$X_p \approx \frac{X_1+X_5}{2} = \frac{X_1+2L+D}{2} \qquad \text{(Eq. 7)}$$

$$\tilde{x} = \frac{D}{2} \qquad \text{(Eq. 8)}$$

where D is the distance traveled in between excitation signals,

$$D = Tv \qquad \text{(Eq. 9)}$$

where T and *v* are the period of the excitation rate (inverse of frequency) and the velocity of the reader with respect to the tag, respectively. Thus,

$$\tilde{x} = \frac{Tv}{2} \qquad \text{(Eq. 10)}$$

As seen in Figure 15, the XR400 RFID reader, with T = 87 milliseconds, reaches ± 1 meter of maximum longitudinal measurement error at approximately 50 miles per hour[11]. It is equally likely that the tag will be read for the first and last time anywhere from zero to D meters into and out of the read field if the velocity of the RFID reader with respect to the tag is constant. Thus, the probability density of the error on the longitudinal measurement is a uniform probability density function with the limits being $\pm\tilde{x}$ about X_p.

[11] There are RFID readers on the market (GAO 216002 RFID reader) with read frequencies as high as 125 Hz, which can attenuate the amount of error by a slightly over one order of magnitude. A reader of this type has maximum errors depicted under the label "GAO 216002 RFID Reader" in Figure 15.

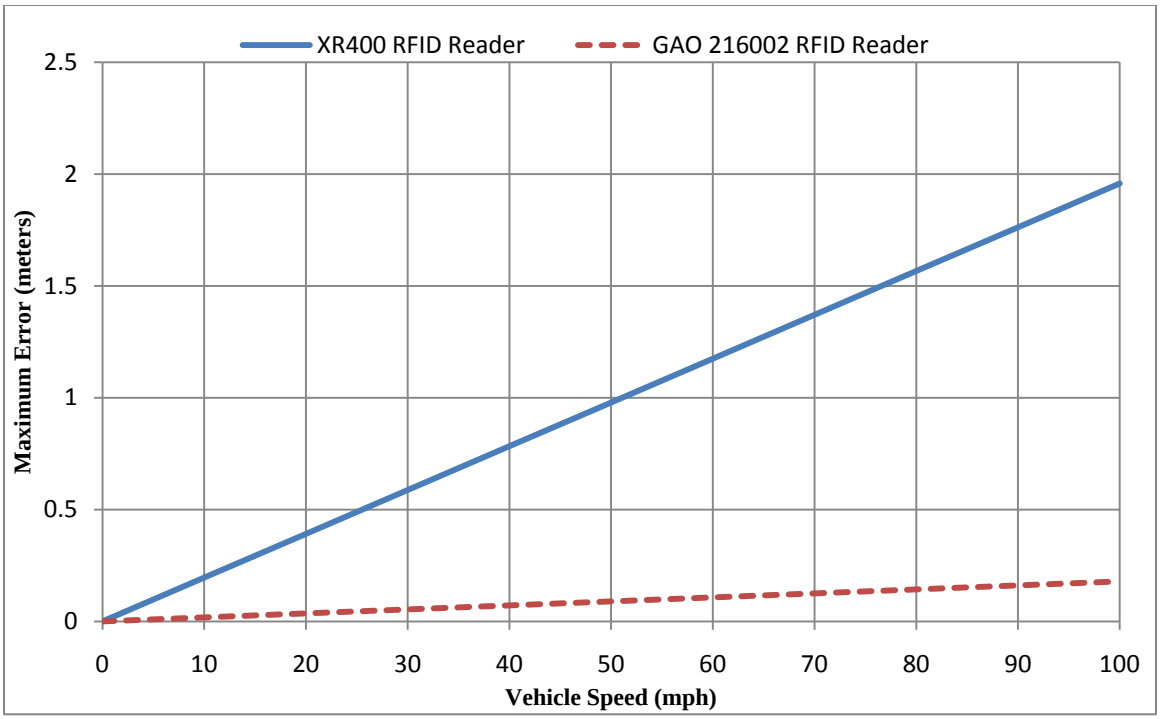

Figure 15. Maximum longitudinal measurement error vs. reader velocity

iv. Attainable Longitudinal Accuracy from Non-contact Odometry

In between measurement updates from VPS, odometry is used to update the longitudinal position. The DRS1000 Delta Speed Sensor from GMH Engineering was the sensor chosen to acquire the speed measurements necessary for implementing odometry. The DRS1000 measures ground speed based on the Doppler shift of the radio waves emitted from the sensor. The DRS1000 operates under the Ka RF frequency band at 35.5 GHz. Detailed specifications for the DRS1000 can be found in Appendix A on page 76. The speed measurements from the DRS1000 cannot be read directly, as it outputs a square wave with a frequency proportional to the speed measurement (100 Hz per MPH). A Weeder Technologies WTPCT-M frequency counter is used to measure the frequency of the output signal from the DRS1000. Specifications for the frequency counter can be found in Appendix A on page 77 (see Figure 24 for hardware integration diagram).

The DRS1000 sensor has a specified accuracy of $\pm(0.34\% + 0.0023\%\ per\ MPH)$ or $\pm(0.34\% + 0.00103\%\ per\ m/s)$ and the frequency counter has a specified accuracy of 0.005%. Thus, the maximum possible error in odometry using the DRS1000 and WTPCT-M frequency counter can be described by coupling the maximum possible error in the velocity with the velocity integration term as shown in the following equation,

$$\tilde{x} = [\pm(0.0034 + 0.0000603v)] \times [vt] \quad \text{(Eq. 11)}\ ^{12}$$

where v and t are the velocity of the vehicle (m/s) and time (seconds) respectively.

[12] Accuracy is also affected by vibration and sensor movement due to vehicle dynamics. These effects are assumed to be small enough to ignore

The odometry error term can also be expressed as a function of the distance between VPS measurement updates, *d* (meters), and the velocity of the vehicle, *v* (m/s), since *d* = *vt*.

$$\tilde{x} = \pm(0.0034 + 0.0000603v)d \qquad \text{(Eq. 12)}$$

Figure 16 shows that the error in odometry grows as the distance since the last update gets larger. This is always an expected occurrence when using a biased sensor for odometry, and is referred to as "drift". This is precisely why the odometry calculation needs to be updated by VPS after a designated distance.

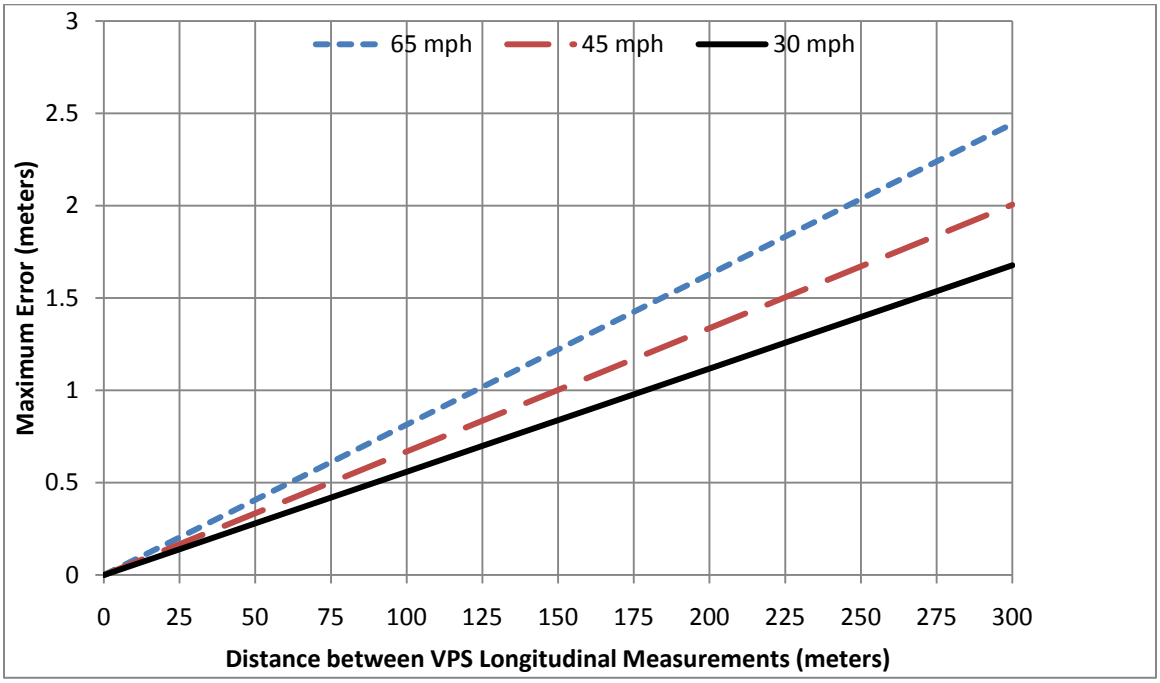

Figure 16. Maximum error in odometry vs. distance between VPS measurements

v. Longitudinal Accuracy from VPS Augmented with Non-contact Odometry

In order to characterize the accuracy of longitudinal measurements obtained by VPS and non-contact odometry, the errors associated with both methods must be combined.

$$\tilde{x}_{vps} = \frac{Tv}{2} \qquad \text{(Eq. 10)}$$

$$\tilde{x}_{odometry} = \pm(0.0034 + 0.0000603v)d \qquad \text{(Eq. 12)}$$

$$\tilde{x}_{total} = \pm\left[(0.0034 + 0.0000603v)d + \frac{Tv}{2}\right] \qquad \text{(Eq. 13)}$$

Figure 17 is a plot of Equation 13 with T equaling 87 ms (XR400 excitation period) and *v* and *t* as the independent variables. The maximum spacing of the RFID tags on the transitway in order to achieve less than 1.05 meters of error is shown to be approximately 29 meters at a vehicle traveling 45 mph (referenced from Figure 17). During testing the spacing was approximately

200 meters, but tags were placed within 29 meters of curb slope changes, such as protected bus stops, and curves to ensure lateral position accuracy.

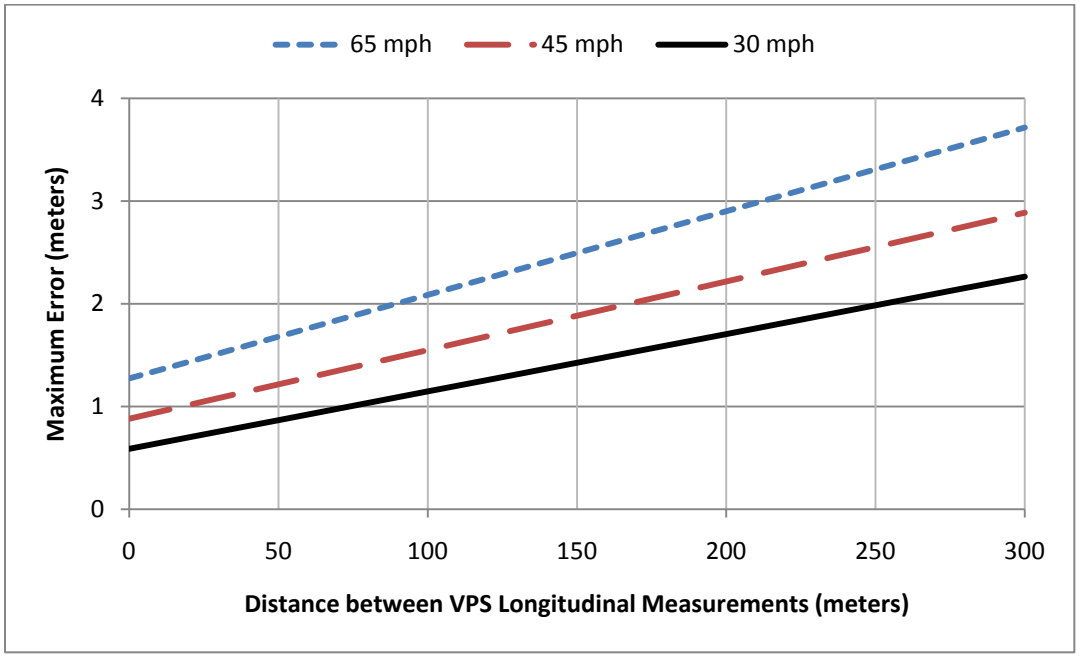

Figure 17. Maximum error in VPS augmented with non-contact odometry versus the distance between VPS updates

vi. Conclusions

The needed longitudinal accuracy of VPS augmented with odometry was determined to be 1.05 meters in order to achieve a desired lateral accuracy of 10 cm. The longitudinal accuracy was then characterized to determine what accuracy is achievable. The accuracy of the VPS longitudinal measurements was shown to be a function of the velocity of the RFID reader with respect to the RFID tags and the frequency at which the excitation signals are sent from the RFID reader. The accuracy of odometry was shown to be a function of the documented bias of the GMH DRS1000 speed sensor and the WTPCT-M frequency counter used to interpret the output from the speed sensor. The dominant error in the longitudinal measurement was shown to be from the VPS measurements. At the vehicle's operating speed of 45 mph and the RFID reader excitation signal period of 87 ms, the VPS measurements accounted for 0.875 meters of the 1.05 meter maximum allowable longitudinal error.

B. LiDAR Curb Detector

i. Test Motivation

The accuracy and reliability of the curb detector were characterized in order to ensure sufficient positioning accuracy can be maintained for use in the lane assistance system described here. The goal of this experiment was to characterize the success rate of the curb detection (measured as a percentage) and the location accuracy as a function of distance between the vehicle and the curb.

ii. Characterization Method

The characterization of the curb detector involves quantifying the accuracy and reliability of the sensor. In order to do this, a vehicle outfitted with a LiDAR sensor and the curb detection software was parked in a stationary position at a given distance from a curb. This was done so that the distance from the vehicle to the curb would be held constant while the curb detection software repeatedly measured vehicle to curb distance. 1000 curb detection measurement samples (measurements of distance from the vehicle to the curb in meters) were collected at approximately 15 hertz for each curb location and each curb shape.

- Independent Variables
  - True Distance from vehicle to curb
  - Curb shape (regular 'square' curb, jersey barrier)
- Dependent variables
  - Mean distance from vehicle to curb measured by curb detector, μ
  - Standard deviation of distance from vehicle to curb measured by curb detector, σ
  - Curb detection success rate (100 * detections / 1000)

Figure 18. (Left) Regular 'square' curb; (right) Jersey barrier

True distance from the vehicle to the curb was difficult to measure at the same accuracy as the LiDAR sensor (on the order of millimeters), so it was left out of the analysis. This is justifiable because the standard deviation of the data sets provide a measure of the repeatability of the overall measurements, which is important because the map database is derived from the same curb detection system. Also, note that the true distances are not the same for the trials with the regular curb shape as those trials with the Jersey barrier (i.e. trial #1's true distance does not equal trial #9's true distance).

iii. Data Analysis

Table 3. Curb detector characterization for regular 'square' curb shapes at different distances

Trial #	μ (meters)	σ (meters)	Curb detection success rate (%)
1	0.2325	0.0033	100.0
2	0.6163	0.0065	100.0
3	1.3316	0.0043	100.0
4	2.6547	0.0045	100.0
5	3.6705	0.0428	100.0*
6	4.2151	0.0073	100.0
7	5.0236	0.0047	99.0
8	5.7352	0.0686	31.0

* -- 4 % false detection

Table 4. Curb detector characterization for Jersey barrier curb shapes at different distances

Trial #	μ (meters)	σ (meters)	Detection %
9	0.2057	0.0017	99.0
10	0.6229	0.0035	99.0
11	1.0386	0.0042	100.0
12	2.0065	0.0112	100.0
13	2.9990	0.0049	100.0
14	4.0416	0.0038	100.0
15	4.6250	0.0066	100.0
16	5.3873	0.0084	88.0

The data shows that the standard deviation of data sets inside of 5 meters is less than 1.2 cm with the exception of trial #5. In trial #5, tall grass formed a "curb" like shelf above the actual curb

and the curb detector falsely indentified the curb in 4% of the 1000 total samples. The likelihood of false detections can be reduced by changing the correlation threshold value, but tradeoffs exist between false detections and detection percentage. The data also portrays that the standard deviation is independent of the curb shape, although the curb detection success rate across the 5 meter range was better for the Jersey barrier. This may have been due to the fact that the Jersey barrier is much larger in size compared to a regular curb, thus making it easier to detect. The histograms for each trial are shown in Appendix A on pages 66 through 74.

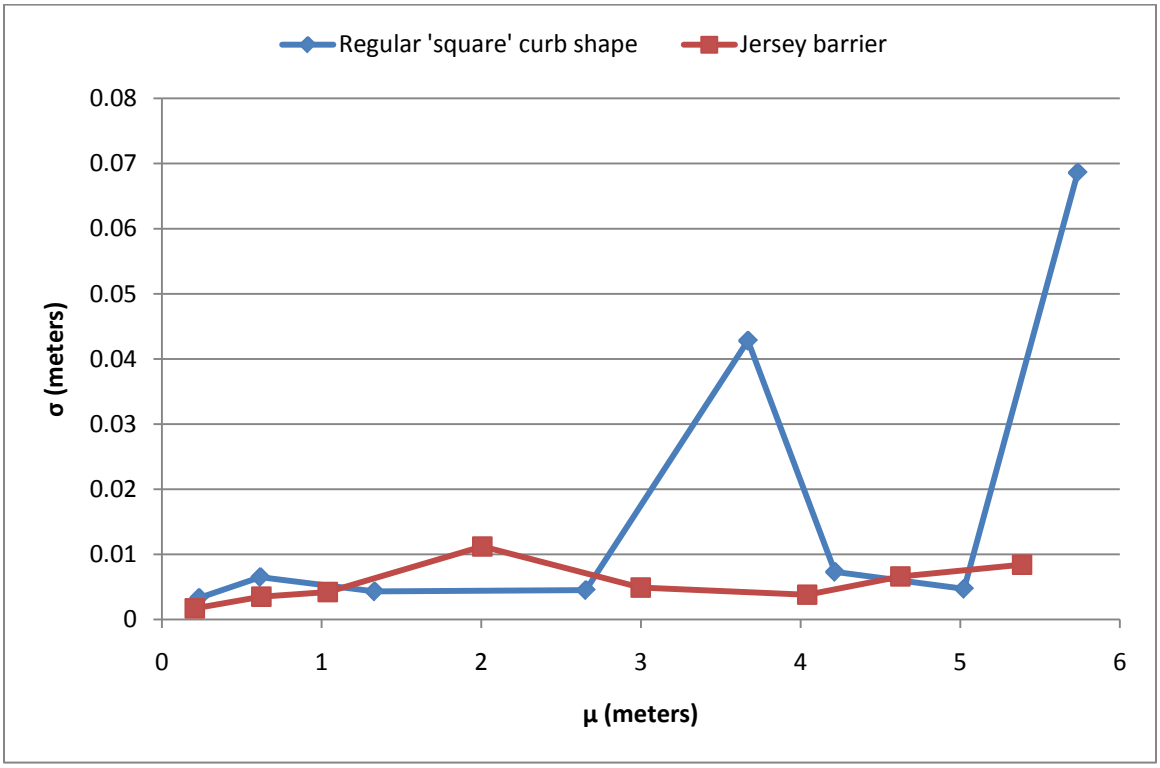

Figure 19. Standard deviation versus mean distance from LiDAR to curb (as measured by curb detector)

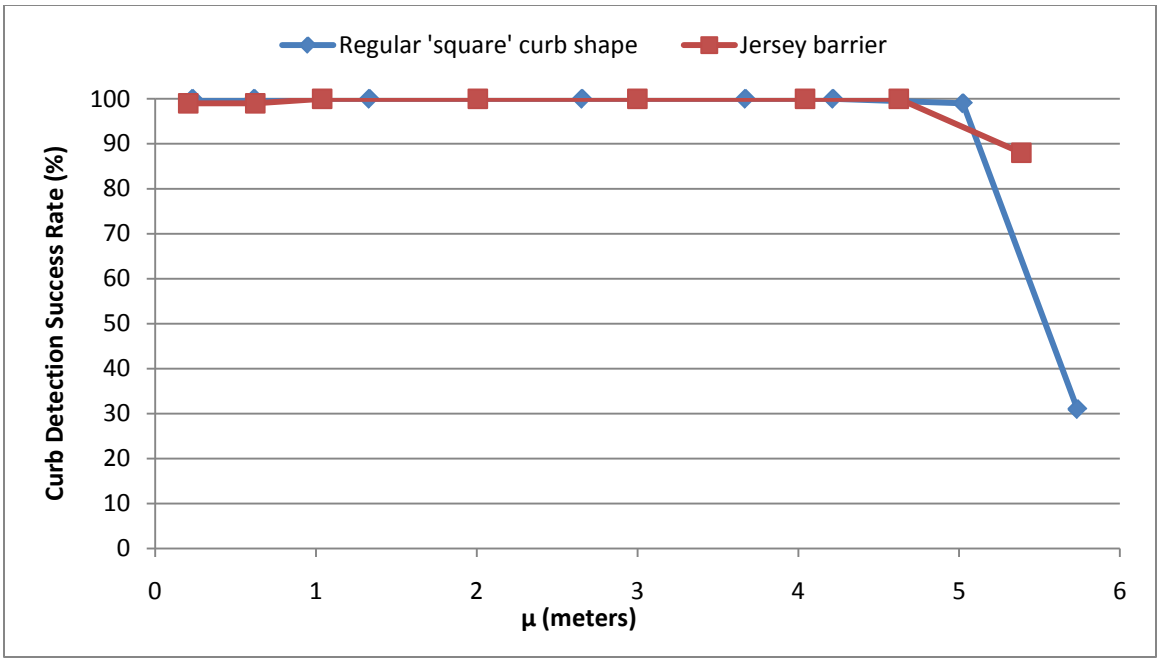

Figure 20. Plot of curb detection success rate versus mean distance from LiDAR to curb (as measured by curb detector)

iv. Conclusions

The data shows that the curb is highly detectable within 5 meters of the vehicle and is located with high accuracy. Outside of 5 meters, the curb detection success rate falls off rapidly. Although it may be possible to increase the curb detection success rate by reducing the correlation, false detections would increase, causing the accuracy of the curb detector to deteriorate.

4. Implementation of the Enhanced VPS Enabled IV Lab Lane Assist Technology on the IV Lab Research Bus

A. Introduction

To demonstrate the performance of the enhanced VPS enabled IV Lab lane assist technology, the system was outfitted on a 40 foot Gillig Phantom transit bus. Two areas where chronic DGPS outages occur were used as proving grounds. The University of Minnesota transitway, which connects the University of Minnesota's Minneapolis and St. Paul campuses, has trees and overpasses that block GPS satellites. The second route was 4th Street in downtown Minneapolis, which has tall buildings that form an "urban canyon" blocking GPS satellites and causing chronic outages for a significant portion of the route. Vehicle data acquisition (VehDAQ) equipment was also installed on the bus to record the performance of the lane assist system on both routes.

B. Proving Grounds

i. University of Minnesota Transitway

Approximately 4 $^2/_3$ miles of the university transitway (see Figure 21) were instrumented for testing the enhanced VPS enabled lane assistance system on the transitway. It was not possible to instrument RFID tags on the roadway itself for the purpose of testing, so RFID tags were placed along each side of the roadway instead as seen in Figure 22[13]. Since only a single lane of travel in each direction was used, this alternative VPS installation is essentially equivalent to the original VPS installation. Twenty eight Motorola Cargo RFID tags were placed on steel light poles, wooden power line poles, and plastic and metal sign posts along the route. A table of the Motorola Cargo RFID tag specifications can be found in Appendix A. Three different curb models were used for curb detection, including Jersey barriers.

[13] RFID tags were placed approximately 200 meters apart

Figure 21. UMN transitway (Background image from Google, Map Data © Google)

Figure 22. RFID tags placed along the transitway (circled)

ii. 4th Street Downtown Minneapolis

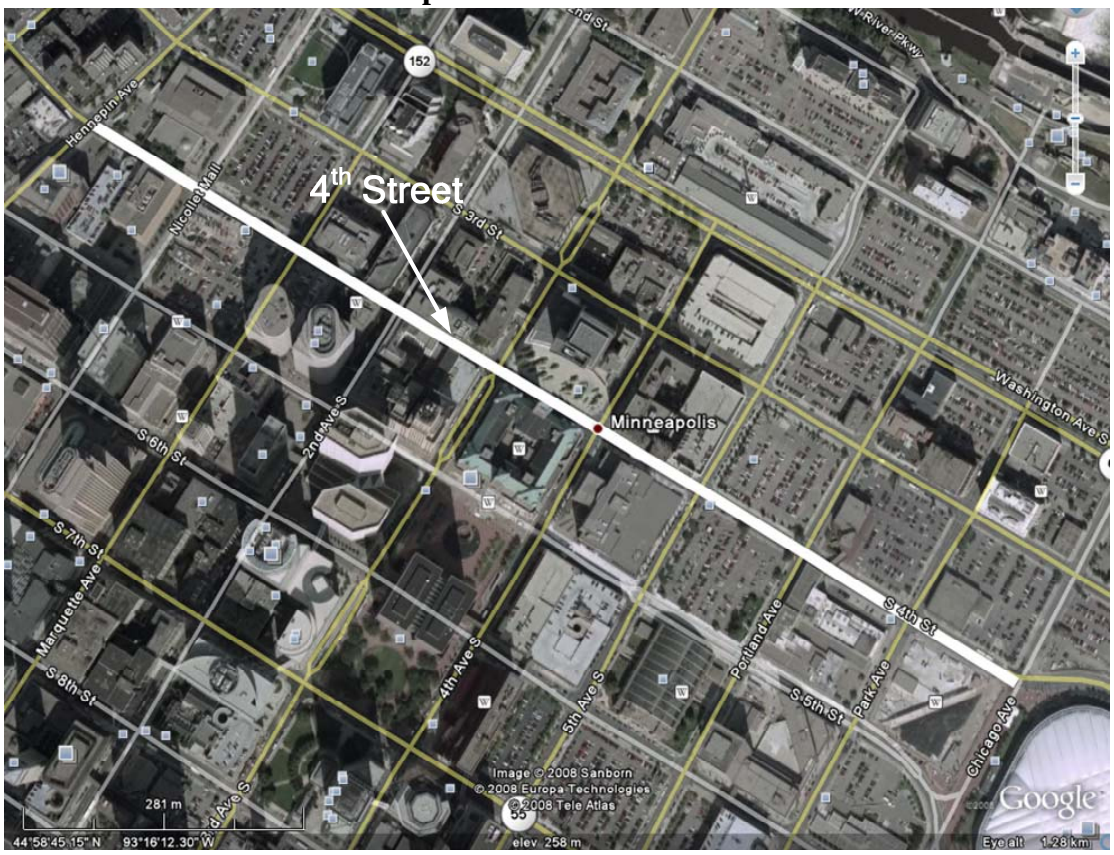

Figure 23. 4th Street downtown Minneapolis (Background image from Google, Map Data © Google)

Nine city blocks on 4th Street between Chicago Avenue and Hennepin Avenue (see Figure 23) were instrumented with eight Motorola Cargo RFID tags spaced approximately 100 meters apart. All of the tags were mounted on metal light poles before intersections. Only one curb model was needed for the curb detector.

C. Hardware Integration onto the IV Lab Research Bus

Figure 24 and Figure 25 describes the hardware configuration used on the research for the prototype system that was characterized in this chapter. Figure 26 describes the hardware installation for the data acquisition equipment used to measure and record the performance of the lane assist system at the test site.

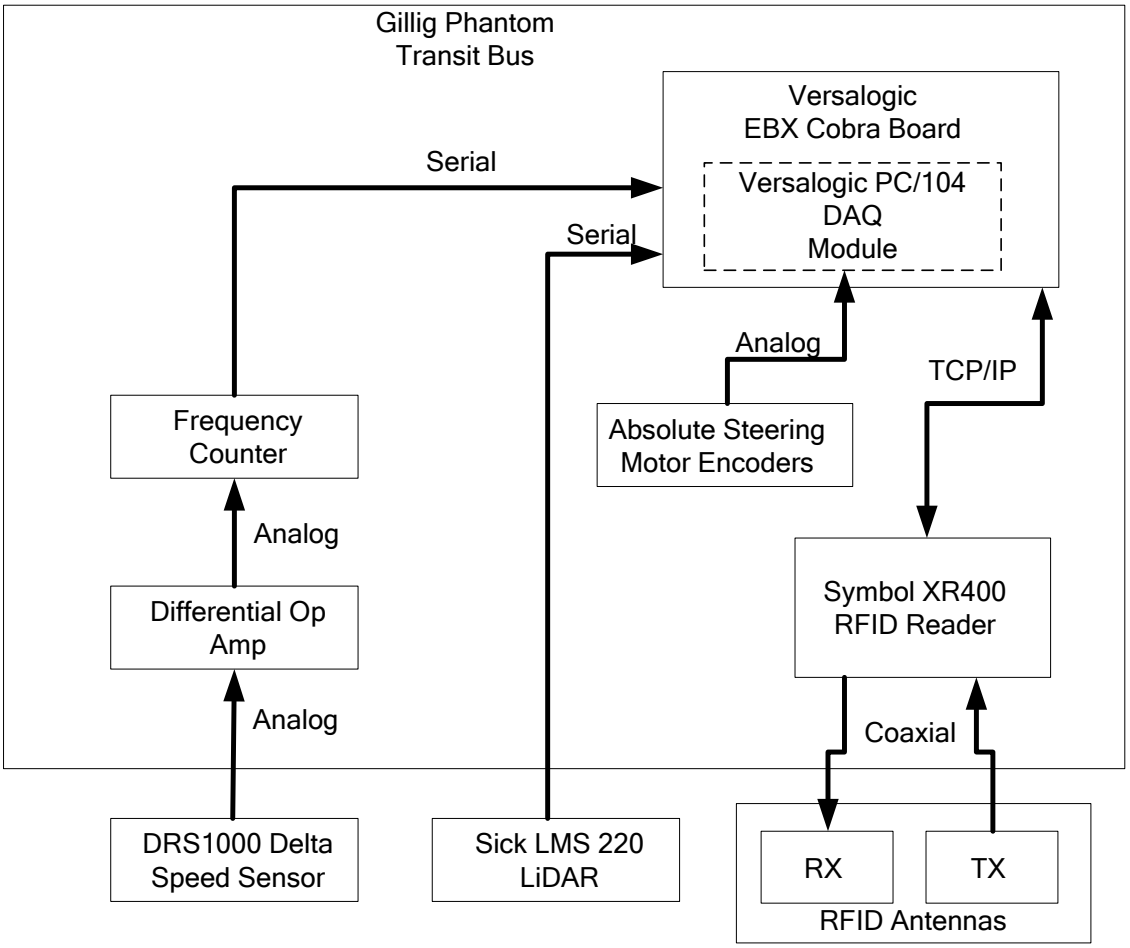

Figure 24. VPS, curb detection and odometry hardware diagram

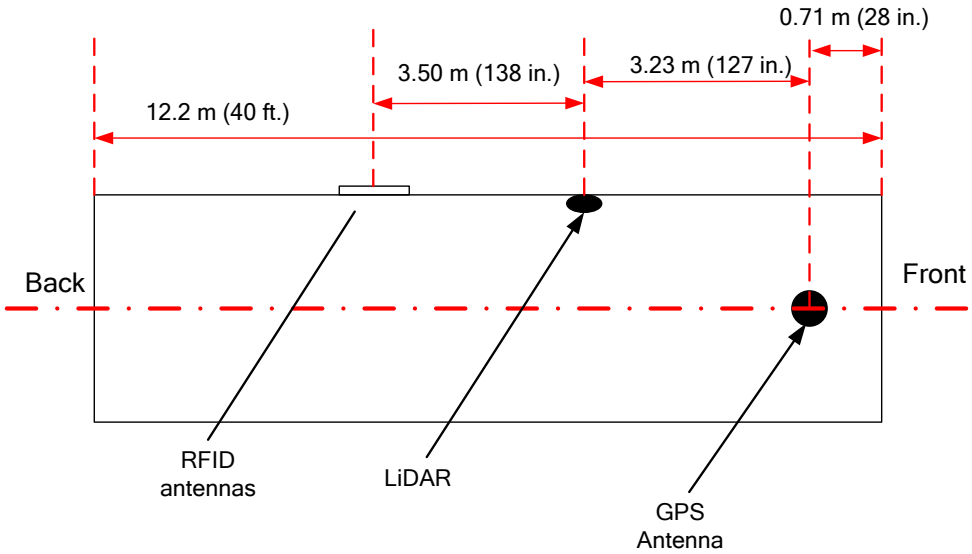

Figure 25. Sensor locations on bus

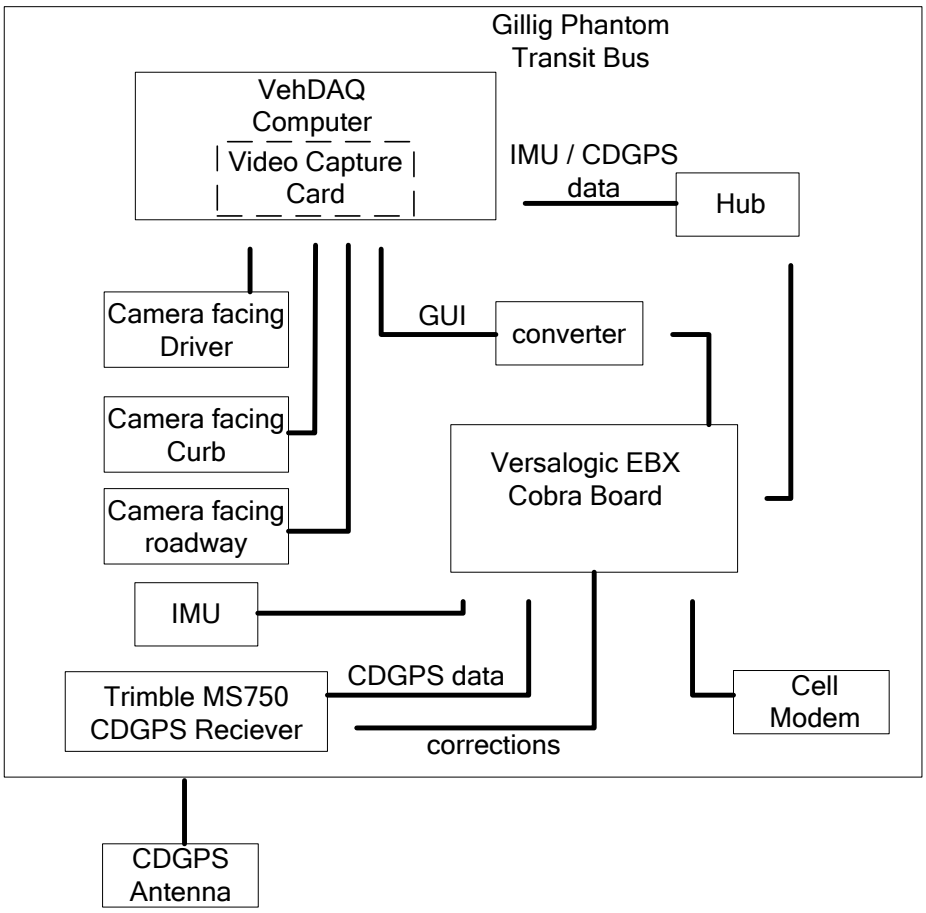

Figure 26. Vehicle data acquisition hardware on bus

D. Characterization of VPS Enabled IV Lab Lane Assist Technology

i. Introduction

The important characteristics of the lane assistance system that were examined to quantify the performance of the enhanced VPS[14] were the lateral position accuracy, ride quality, and the automated lane-keeping provided by the haptic feedback in the steering wheel. The lateral positioning, namely the lateral offset between the vehicle and lane centerlines, is compared between the enhanced VPS and high accuracy DGPS. Ride quality is quantified by lateral acceleration measured with an inertial measurement unit. Lateral acceleration is compared between the automated lane-keeping of the VPS lane assistance system, the DGPS lane assistance system, and a manually operated vehicle. The accuracy of the feedback from the lane assistance system using the enhanced VPS is demonstrated by the automated lane-keeping of the bus via the haptic feedback in the steering wheel.[15]

[14] Enhanced VPS refers to VPS augmented with odometry and LiDAR curb detection for complete in-lane level positioning

[15] A video demonstrating the lane keeping ability of the automated steering is available upon request to the author

ii. Data Acquisition

The following data was acquired in order to characterize the VPS lane assistance system.

- From the DGPS receiver (Trimble #MS750)
  - Position
  - Timestamp (μs)
  - Quality
    - 4 – Real Time Kinematic (RTK) fixed solution
    - 3 – RTK floating solution
    - 2 – DGPS solution
    - 1 – Autonomous solution (no correction)

- From the Enhanced VPS
  - Lateral Offset
  - Timestamp (μs)
  - Distance from LiDAR sensor to curb
- From the IMU (Crossbow DMU-HDX)
  - Lateral acceleration
  - Timestamp (μs)
- From the VehDAQ
  - Three channels of video (frontal shot of driver, view of curb, driver's view of road)
  - One channel of VGA output displaying lane assistance system GUI
  - Timestamp (μs)

The DGPS receives corrections from a Trimble Virtual Reference System (VRS) at one hertz via cellular modem[16] connection with the Minnesota Department of Transportation server. The mean and standard deviation of the error in dynamic DGPS position estimates was previously characterized in [17], and a table summarizing the results is shown in Table 5.

Table 5. Dynamic DGPS accuracy with long baseline VRS corrections and Trimble MS750 DGPS receiver

Speed (KPH)	Mean error (cm)	Standard deviation (cm)
16	9.4	8.9
32	7.1	4.6
48	7.3	4.5

iii. Lateral Position Estimate Accuracy

The lateral position estimate is a very important parameter of the enhanced VPS to characterize. For a lane assistance system, having an accurate measure of where the vehicle is positioned

[16] Uses AT&T 3G service

laterally in the lane is of utmost importance. The lateral offset measurements provided by the enhanced VPS were compared with high accuracy lateral offset measurements post-processed from DGPS data[17]. In order to post-process the vehicle's lateral offset, DGPS position data was collected during the same mapping run (when the vehicle is assumed to drive down the center of the lane) used to derive the enhanced VPS map database. This ensures that the lateral offsets calculated from the VPS system and those post-processed from the DGPS position data are from the same lane center positions. Subsequent trial runs were then driven and DGPS trial run data was collected. When each trial run DGPS data point is collected the associated lateral offset measured by the enhanced VPS is also collected. When the lateral offset is post-processed from the trial run data point and the DGPS mapping data, it is compared with the associated lateral offset measured by the enhanced VPS to determine the lateral error from the VPS offset measurement. The lateral error of the enhanced VPS is defined as the difference between the lateral offset measured by the enhanced VPS and the lateral offset post-processed from the DGPS map and trial run data.

$$lateral\ error = lateral\ offset_{vps} - lateral\ offset_{DGPS}$$

Only the DGPS data that had the highest quality (fixed quality) was used in the comparison so that the accuracy of the comparison was not mitigated.

Table 6. In-lane level position accuracy experimental results

	Trial run #1	Trial run #2
Mean lateral error	0.004 m	-0.004 m
Standard deviation of lateral error	0.046 m	0.039 m
Mean speed	12.92 m/s (28.90 mph)	10.45 m/s (23.37 mph)
Standard deviation of speed	1.49 m/s (3.33 mph)	1.85 m/s (4.14 mph)
Mean distance from LiDAR to curb	1.682 m	1.558 m
Standard deviation of distance from LiDAR to curb	0.542 m	0.486 m
Number of samples	832	1267

Speed was the independent variable that was varied between the two runs. The test site's speed limit and heavy traffic limited the amount the speed could be varied, so it is hard to extrapolate the lateral error as a function of speed. The distributions of the lateral error for trial run 1 and

[17] An explanation of computing based on DGPS position data can be found in Appendix A.

trial run 2 are shown in Figure 27 (top) and Figure 29 (top). The distribution of the distance from the LiDAR to the curb is shown in Figure 28 (top) and Figure 30 (top) to show the variations in this distance during the data collection. There are two distinct groupings in these histograms, which are due to the typical distance a regular curb shape is from the lane centerline and the distance a Jersey barrier is from the lane centerline. On the transitway, the Jersey barriers are located at a greater distance from the lane centerline (~2.4 meters) as opposed to a regular curb (~1.3 meters). The plots of lateral offset obtained from both the DGPS and the enhanced VPS are shown in Figure 28 (bottom) and Figure 30 (bottom). These plots show the lateral offsets from VPS and DGPS that were used to compute the lateral errors in the histograms of Figure 27 (top) and Figure 29 (top).[18] Notice that when there is a float DGPS solution there is a noticeable increase in the amount of lateral error. This is assumed to be the caused by a low accuracy DGPS solution, thus these lateral offsets were not included in the lateral error data sets. The largest lateral error standard deviation of 0.046 meters is less than half of the desired accuracy goal of 1 decimeter, which implies that the system will achieve an accuracy of 10 cm at the 95% statistical level associated with two standard deviations.

[18] Except for the DGPS float position solutions

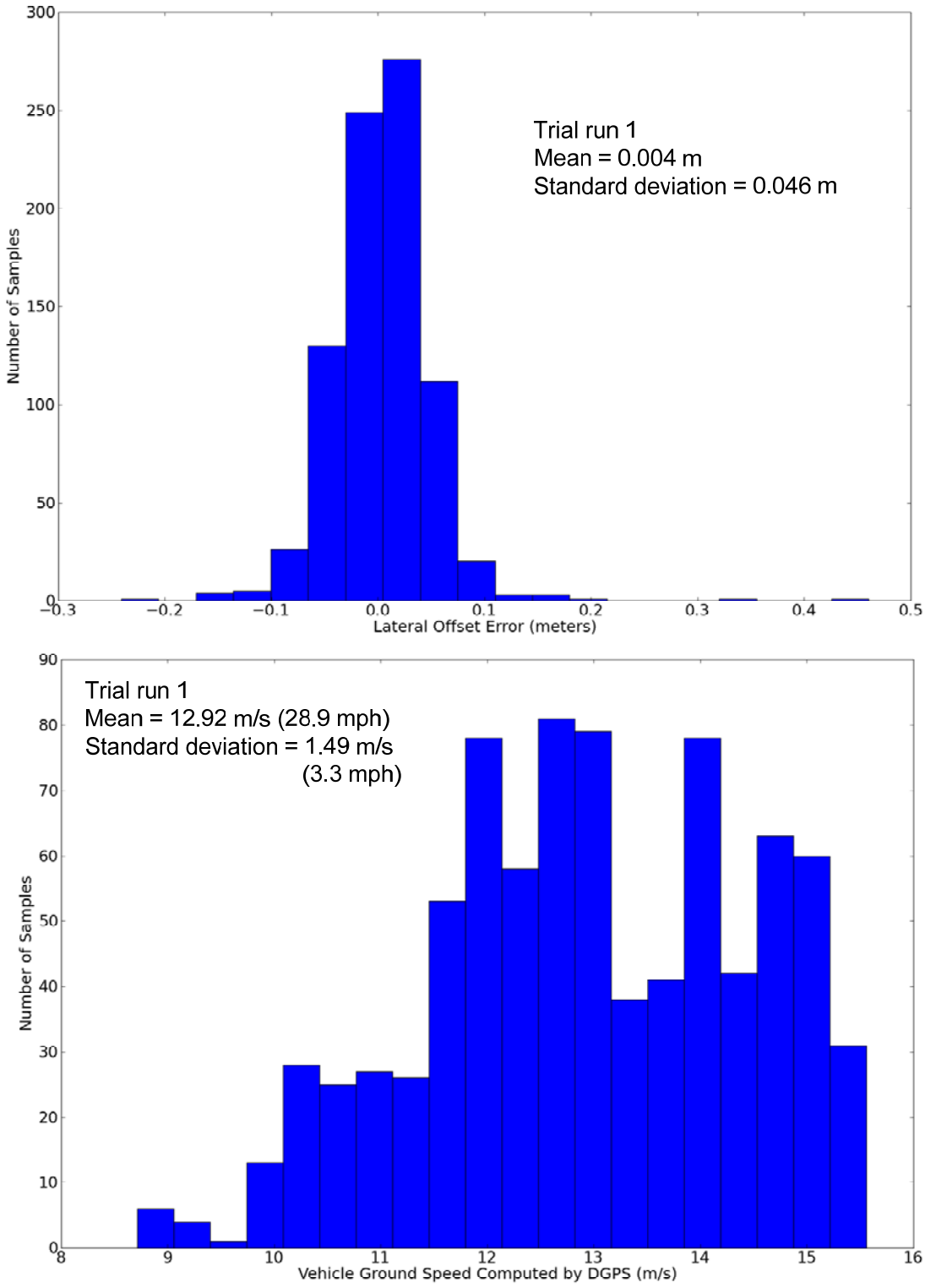

Figure 27. Histogram of the enhanced VPS lateral error for trial run 1 (top); histogram of vehicle ground speed for trial run 1 (bottom)

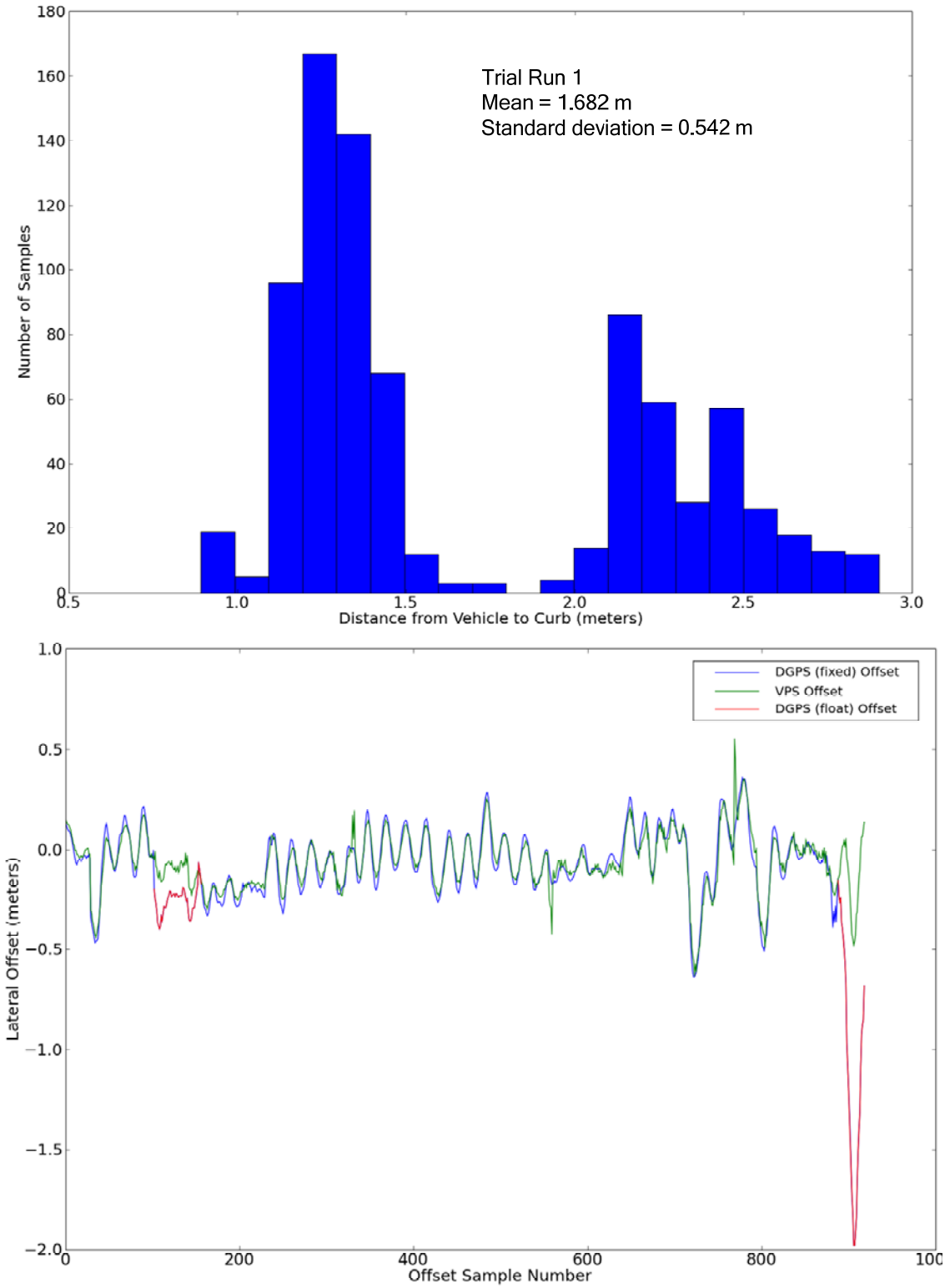

Figure 28. Histogram of distance from the vehicle to the curb for trial run 1 (top), plot of VPS and DGPS computed lane offsets for trial run 1 (bottom)

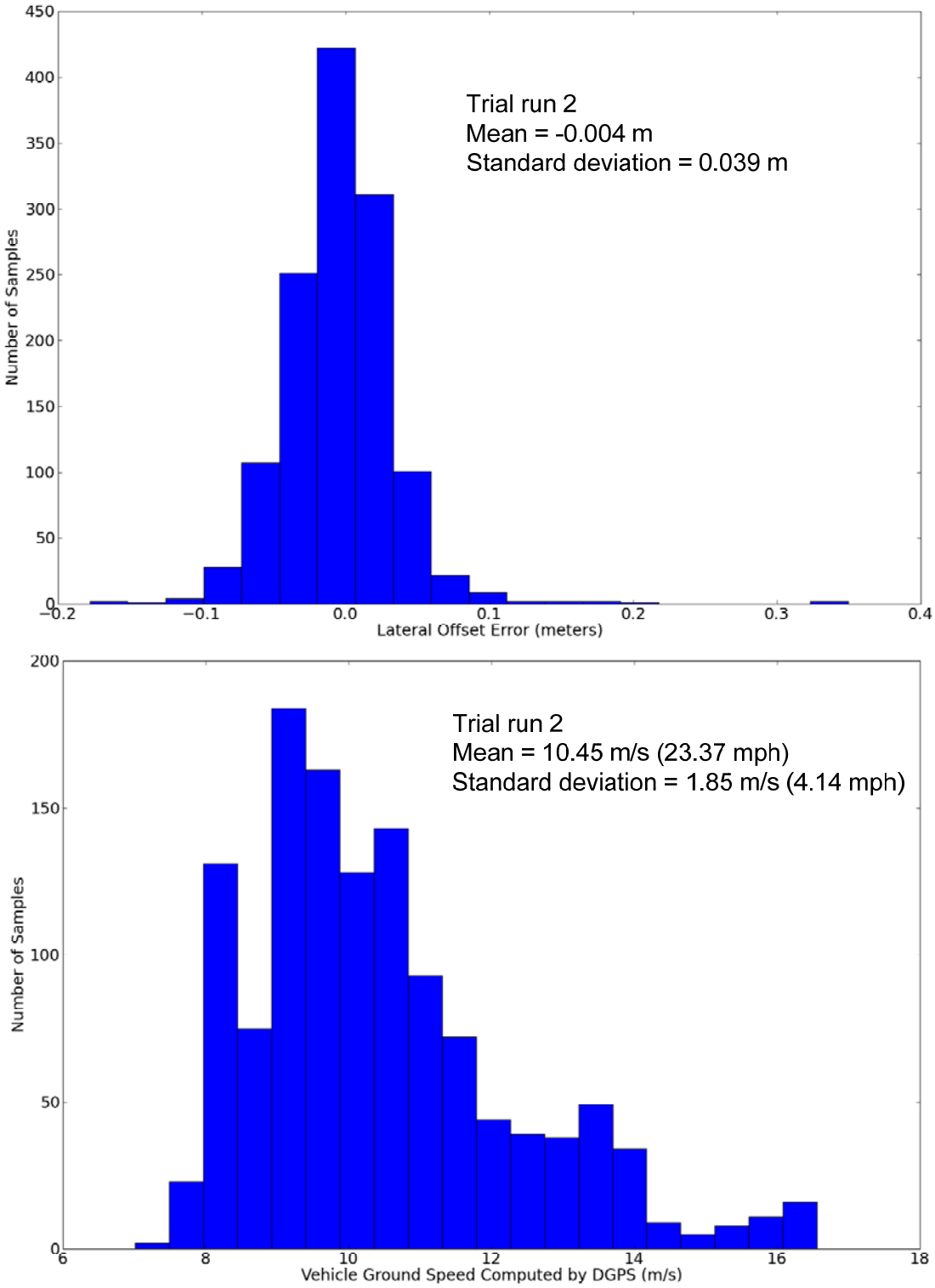

Figure 29. Histogram of the enhanced VPS lateral error for trial run 2 (top), histogram of vehicle ground speed for trial run 2 (bottom)

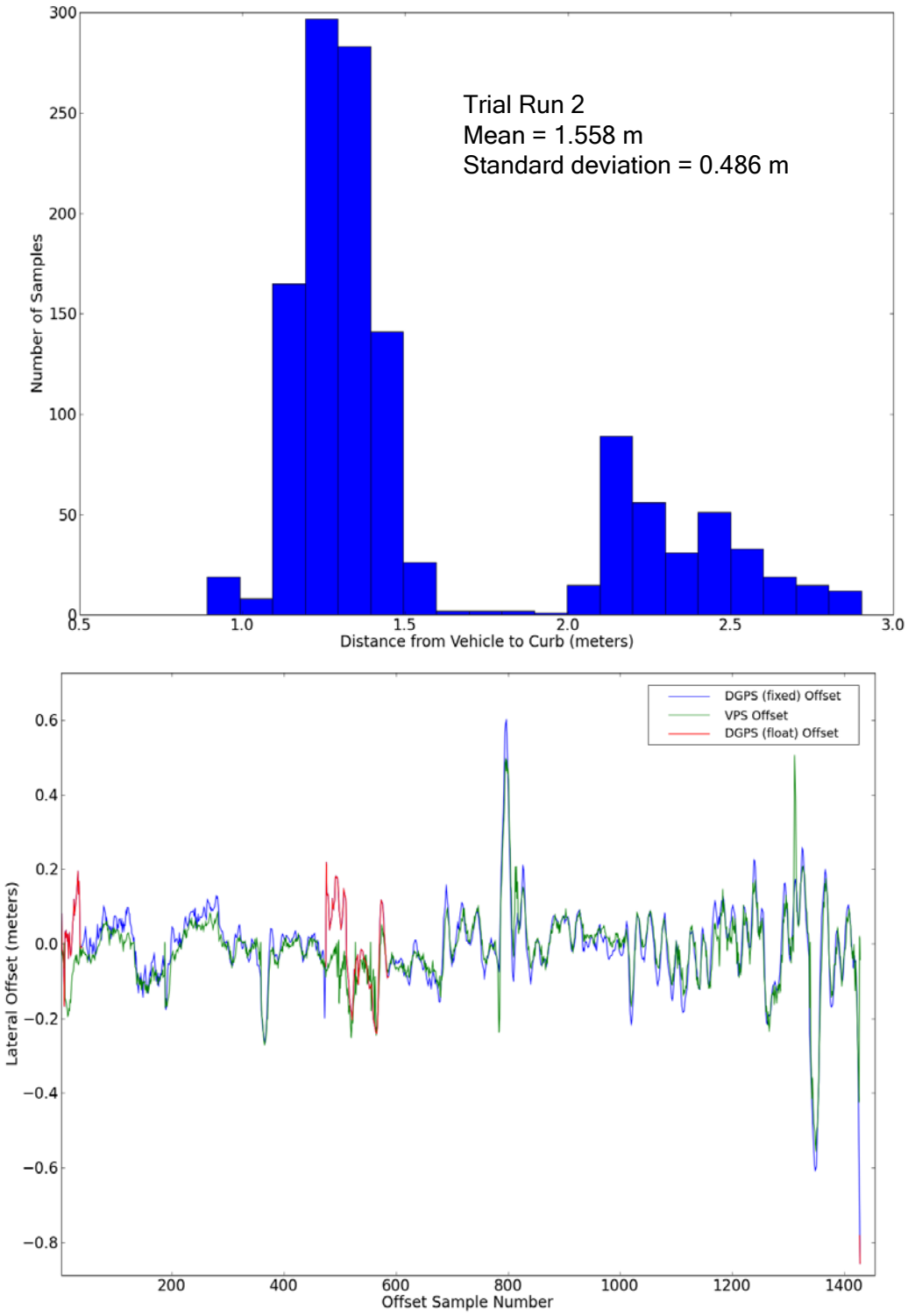

Figure 30. Histogram of distance from the vehicle to the curb for trial run 2 (top), plot of VPS and DGPS computed lane offsets for trial run 2 (bottom)

iv. Ride Quality

Ride quality is also a very important characteristic of the VPS enabled lane assistance system. The operator and the passengers must feel comfortable riding in a vehicle with haptic feedback in the steering wheel. If the feedback is too aggressive or unstable, it will only increase the stress of the operator and passengers in the vehicle. Ride quality, in this work, is quantified by the lateral acceleration inside the vehicle measured by an inertial measurement unit (IMU). Measured lateral accelerations are compared between three modes of operation: the VPS enabled lane assistance system providing the automated steering; the DGPS enabled lane assistance system providing the automated steering; and manually operated steering. All data sets were collected on a straight segment of roadway in order to remove any bias acceleration from road curvature.

Table 7. Tabulated results for ride quality experiment

Mode	Mean Lateral Acceleration (m/s^2)	Standard Deviation of Lateral Acceleration (m/s^2)	Distance Traveled	Average Speed
VPS Enabled	0.216	0.264	384 meters (0.24 miles)	11.6 m/s (25.9 mph)
DGPS Enabled	0.186	0.270	384 meters (0.24 miles)	13.7 m/s (30.6 mph)
Manually Operated	0.225	0.337	341 meters (0.21 miles)	12.6 m/s (28.2 mph)

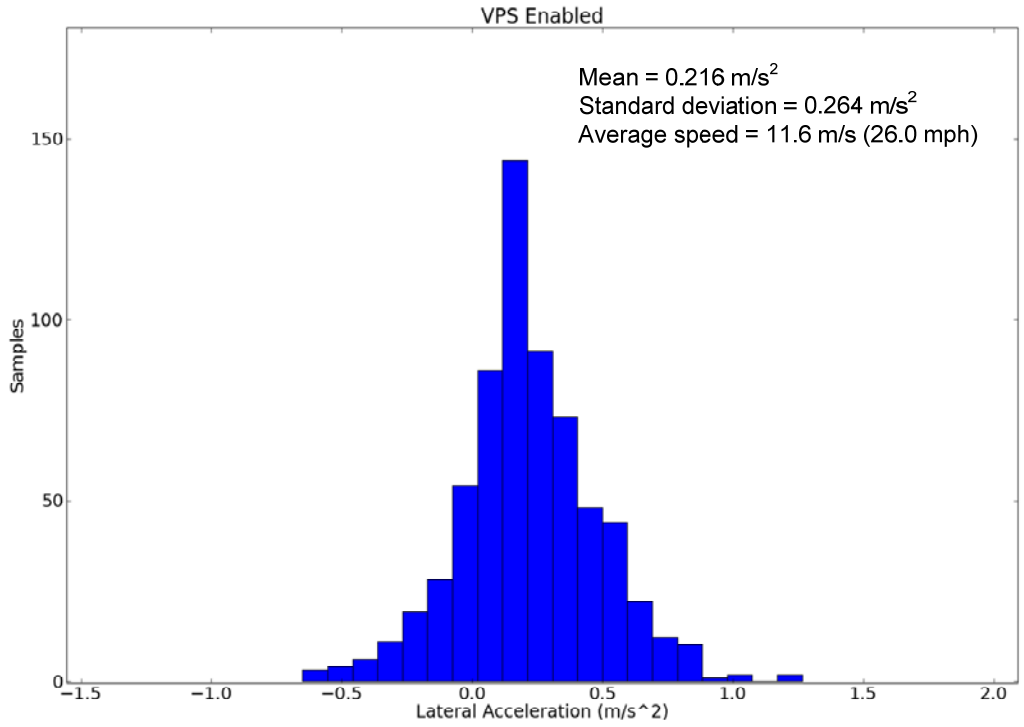

Figure 31. Lateral acceleration during VPS enabled lane assistance system operation

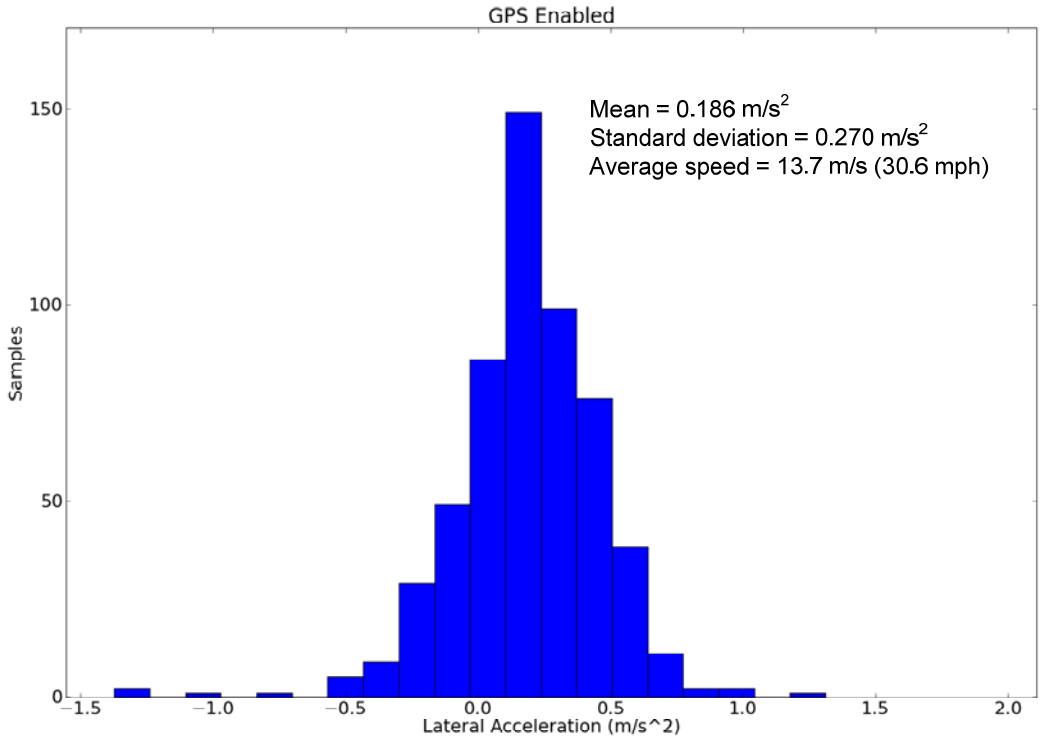

Figure 32. Lateral acceleration of GPS enabled lane assistance operation

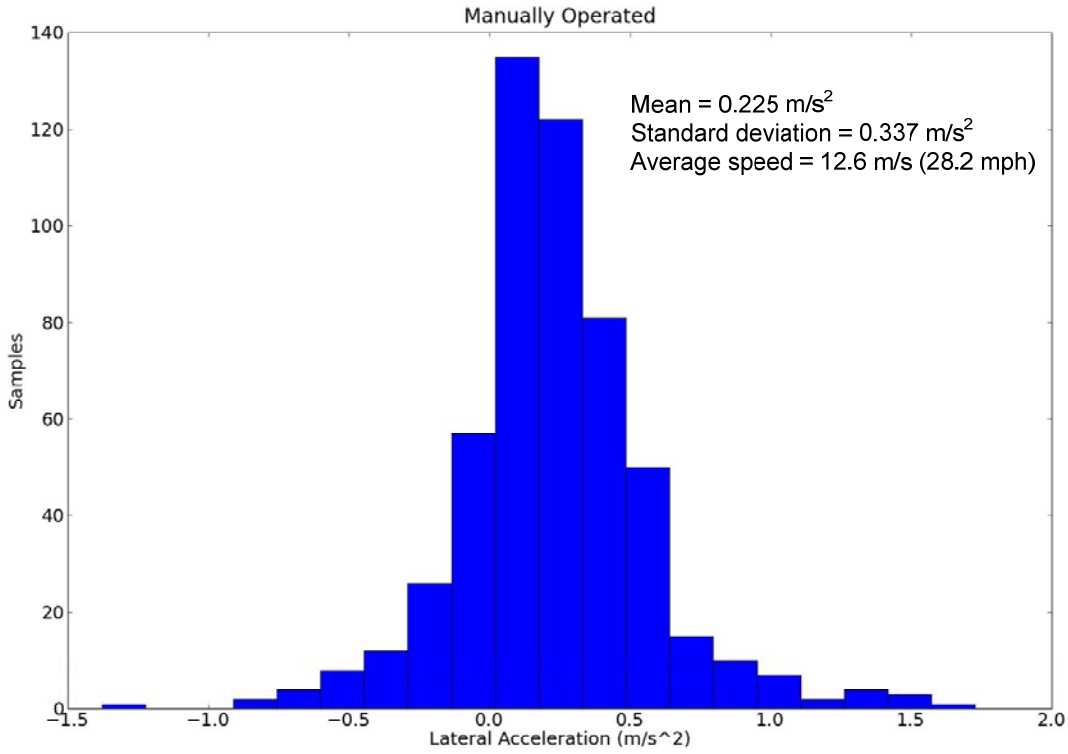

Figure 33. Lateral acceleration of manually operated vehicle

The differences between the mean lateral acceleration for the VPS enabled system and the other modes of operation were under three thousandths of a G, which is virtually indistinguishable. For all intensive purposes the ride quality between the three modes of operation are equal.

v. Automated Lane-Keeping

The haptic feedback through the steering wheel provides a level of automated lane keeping for the bus when the lane assist system is operating. The feedback is controlled by a steering controller within the lane assist system.

The steering controller's input is the lateral lane offset and feed-forward steering angle and the output is the motor angle that corresponds to the desired steering angle to keep the vehicle in line with the center of the lane. The desired steering angle is determined by the sum of two PID control loops:

1. Lateral offset is the error term in the first PID control loop
2. Heading angle with respect to the lane center id the error term in the second PID control loop

The lateral offset is fed into the steering controller, but the heading angle is estimated from successive lateral offset measurements from the enhanced VPS. The heading angle, θ, is illustrated in Figure 34 and shown in equation 14.

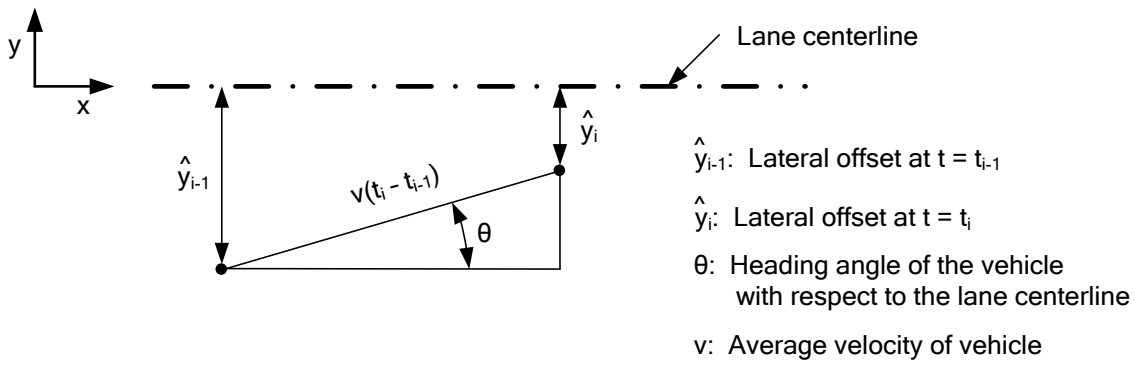

Figure 34. Illustration of heading angle with respect to the lane centerline

$$\theta = \sin^{-1}\left[\frac{(\hat{y}_i - \hat{y}_{i-1})}{v(t_i - t_{i-1})}\right] \qquad \text{(Eq. 14)}$$

The heading angle is susceptible to errors in the lateral offset measurements provided by the enhanced VPS, so a smoothing filter (using successive heading estimates) can provide a more accurate heading angle estimate. Of course, like any smoothing filter there is a tradeoff between lag and noise cancellation in the estimate desired. The heading angle provides increased robustness in the performance of the steering controller.

Figure 35 shows how the haptic steering information flows from the enhanced VPS to the steering motor.

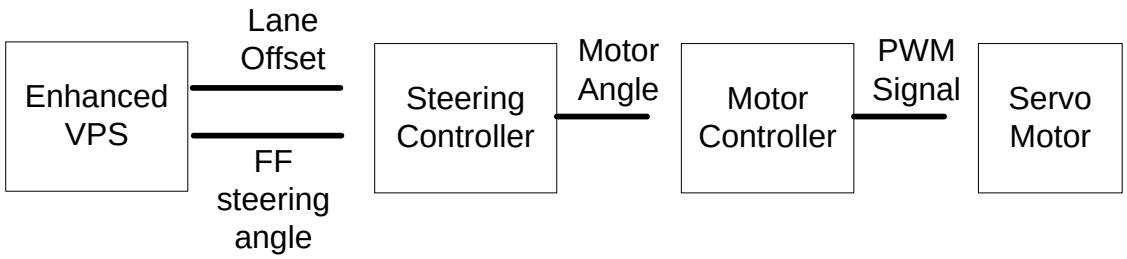

Figure 35. Haptic feedback flowchart

Lateral offset data was collected during VPS enabled lane-assist operation of the bus to quantify the performance of the automated lane-keeping. 2,099 data points were collected over two trial runs on the university transitway from Minneapolis to St. Paul. The distributions of the lateral offsets are shown in Figure 36 and Figure 37.

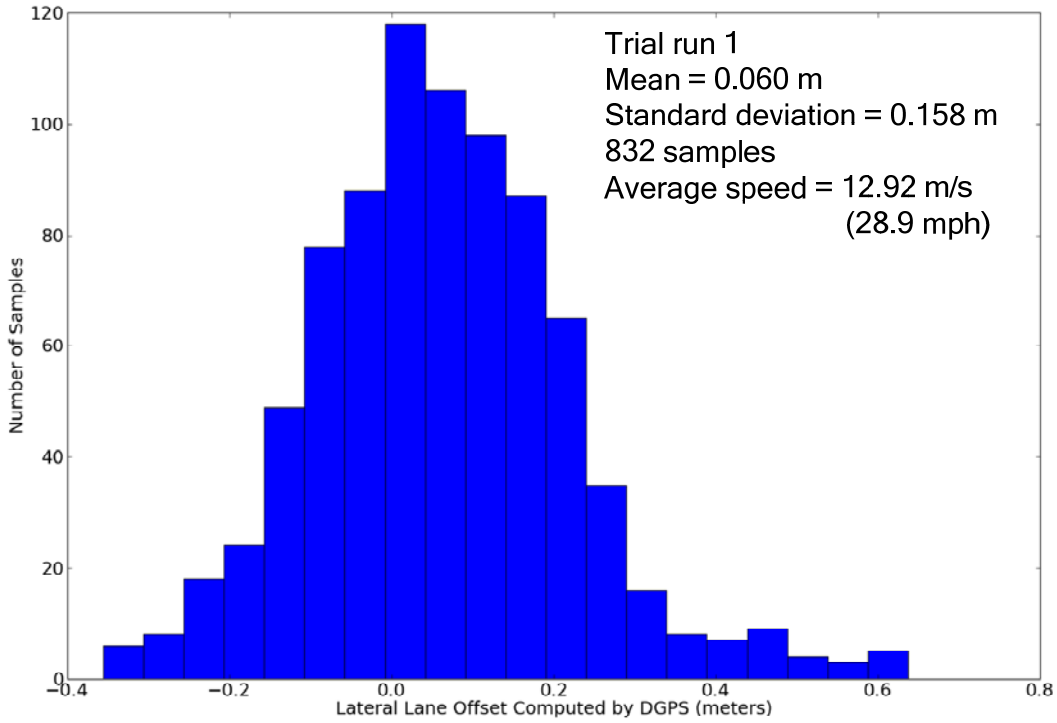

Figure 36. Lateral offset for trial run 1 during VPS enabled lane assistance operation

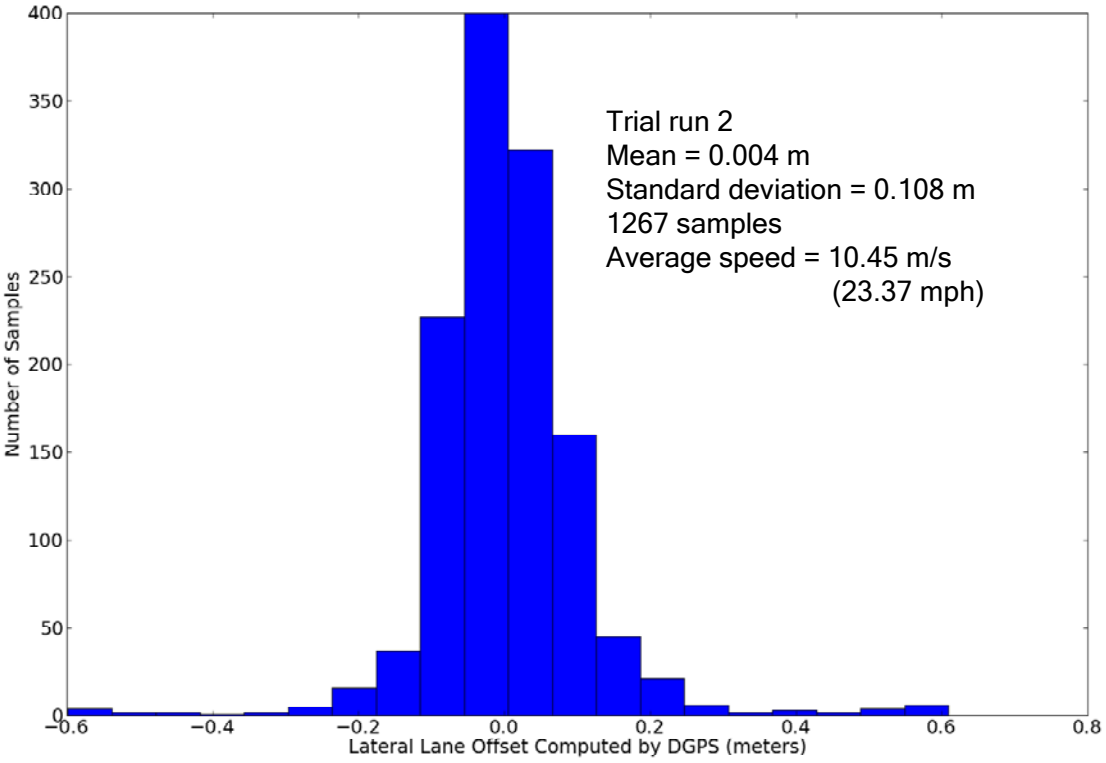

Figure 37. Lateral offset for trial run 2 during VPS enabled lane assistance operation

The research bus is 2.59 meters wide and operates in lanes as narrow as 3.05 meters. This leaves 0.23 meters on each side of the vehicle. Although the data reflects that the lane boundary limits are at most 1 ½ standard deviations from the mean, the lane boundaries are still crossed at times. This is assumed not to happen from position errors provided by the enhanced VPS, but from sub-optimal steering controller performance.

vi. Conclusions

The experimental data demonstrated that the in-lane level position estimates from the enhanced VPS were accurate enough to support a lane assistance system. The ride quality during automated lane-keeping was shown to be indistinguishable from human driving or from a high accuracy DGPS lane assistance system. Also, during automated lane-keeping, the lateral lane offsets were within 2 standard deviations of the lane boundaries of a ten foot lane. Increased performance is assumed to be obtainable from automated lane-keeping by optimizing the steering controller.

5. Conclusion

A. Overview

The goal of this work was to fuse VPS, LiDAR curb detection, and odometry into an enhanced VPS, capable of providing highly accurate lateral, "where in lane," position for the IV Lab lane assist system. The enhanced VPS can be relied upon when DGPS outages occur in environments where tall structures degrade or block satellite signal quality, which primarily occurs in urban areas.

Traffic congestion is at an all time high, and has been increasing rapidly over the past 20 years. Bus Rapid Transit (BRT) systems are a low cost and efficient solution to traffic congestion. Lane assistance systems provide an important benefit to BRT systems, where bus-dedicated lanes and road shoulders are narrower than general traffic lanes. The ability to operate the lane assistance system in urban as well as suburban and rural environments is crucial to the robustness and flexibility of the system.

Chapters two through four examined and characterized the enhanced VPS system, including basic VPS, LiDAR curb detection, and odometry, as well as an implementation of the IV Lab lane assist system using the enhanced VPS on the IV Lab research bus. These results are briefly summarized in this chapter.

B. Enhanced VPS

The IV Lab previously developed a Vehicle Positioning System (VPS) that provides lane level position using RFID tags placed along (as well as on or in) the road. The RFID tags store road, lane, and longitudinal position information in this project. Odometry was implemented to provide longitudinal position estimates between RFID tag reads, thus providing higher frequency position estimates than basic VPS. In order to provide the "where in lane" level position, basic VPS was fused with LiDAR curb detection. This allows the vehicle's position to be sensed not only in a lane, but at a specific position within the lane. When basic VPS is fused with LiDAR curb detection and odometry, enhanced VPS is realized.

C. Characterization of Sensors

i. VPS Augmented with Odometry

In this system, the VPS is augmented with odometry in order to provide accurate longitudinal position estimates to ensure that the correct lane center position, feed-forward steering angle, and curb shape is queried from the map database. If the lateral distance between the curb and lane center changes or a curve in the road is present, longitudinal position errors will provide inaccurate map database information and lead to lateral position errors. The required longitudinal position accuracy was derived and is represented in the following equation,

$$0 = \tilde{x}^2 + \frac{2m(r-\tilde{y})}{m^2+1}\tilde{x} + \frac{(\tilde{y}-2r)}{(m^2+1)}\tilde{y} \qquad \text{(Eq. 4)}$$

where $\tilde{y}$, $\tilde{x}$, and r are the lateral position error, longitudinal measurement error, and the radius of curvature of the road, and m is the slope of the curb[19]. The maximum longitudinal measurement error, $\tilde{x}$, to insure a lateral position accuracy of $\tilde{y}$ can be solved for with $\tilde{y}$ = 10 cm, r = 50 meters (typical radius of an interstate clover leaf) and m = 0.0852. The slope of the curb, m, was chosen based on measuring extreme curb slopes on the university transitway, which was used as the proving grounds for this project. From these assumed values, the maximum error allowable in a longitudinal position measurement is 1.05 meters.

Next, the longitudinal accuracy of VPS augmented with odometry was characterized to determine if it could meet the requirements. The longitudinal position measurement errors for VPS and odometry were found separately and combined, and this maximum error is represented by the following equation,

$$\tilde{x}_{total} = \pm\left[(0.0034 + 0.0000603v)d + \frac{Tv}{2}\right] \qquad \text{(Eq. 13)}$$

where v is the velocity of the vehicle in meters per second, d is the distance in meters between VPS updates, and T is the period in seconds of which excitation signals are transmitted by the RFID reader (period is the inverse of frequency). The distance between VPS tag updates was determined to be approximately 29 meters in order to achieve longitudinal accuracies within the 1.05 meter requirement. This was determined based on the characteristics of the Symbol XR400 RFID reader, DRS 1000 Doppler speed sensor, the road geometry of the university transitway, and the maximum operating speed of 45 MPH. The dominant error in the longitudinal measurement was shown to result from the VPS measurements. At the vehicle's operating speed of 45 mph and the RFID reader excitation signal period of 87 ms, the VPS measurements accounted for 0.875 meters of the 1.05 meter maximum allowable longitudinal error. This error can be reduced by an order of magnitude with, for example, the GAO 216002 RFID reader, which has a higher excitation signal frequency than the XR400. The distance between the VPS measurement updates were increased to up to 200 meters during testing on the university transitway and on 4th Street. This was allowable because VPS tag updates were provided near curves in the road and areas where the distance from the curb to the lane center changed.

ii. LiDAR Curb Detector

The characterization of the curb detector involves quantifying the accuracy and reliability of the sensor in the lateral operating range, which was chosen to be within 5 meters of the curb based on the results of the characterization in chapter three. In order to do this, a vehicle outfitted with a LiDAR and the curb detection software was parked stationary at a given distance from the curb. This was done so that the distance from the vehicle to the curb would be held constant while the curb detection software repeatedly measured vehicle to curb distance. 1000 curb detection samples (measurements of distance from the vehicle to the curb in meters) were collected at approximately 15 hertz for each curb location. The mean, μ, and standard deviation, σ, were computed for each data set and the detection percentage was also quantified. The data showed that the standard deviation of data sets in the operating range were less than 1.2 cm with the exception of one data set where the curb detector had a false positive 4% of the time increasing the standard deviation to 4 cm. The likelihood of false detections can be reduced by

[19] The slope of the curb is defined as the ratio of the change in lateral distance from the lane center to the curb over the change in longitudinal position

changing the correlation threshold value, but tradeoffs exist between false detections and detection percentage. The data also shows that the standard deviation is independent of the curb shape, although the curb detection success rate across the 5 meter range was better for the Jersey barrier. This may have been due to the fact that the Jersey barrier is much larger in size compared to a regular curb, thus making it easier to detect.

D. Implementation of the Enhanced VPS Enabled IV Lab Lane Assist Technology on the IV Lab Research Bus

The VPS enabled IV Lab lane assist system was outfitted on the IV Lab research bus. The lane assistance system was characterized based on three characteristics.

1. lateral position accuracy
2. ride quality
3. automated lane keeping

The lateral offset estimates from the enhanced VPS were compared to estimates post-processed from high accuracy DGPS position data. The data from both trials show that the mean difference between the lateral offset found by the enhanced VPS and that found by DGPS is under 0.4 cm with a standard deviation under of 4.6 cm.

The ride quality of the research bus was characterized when automated lane-keeping was operating using enhanced VPS, compared to GPS as well as when manually operated. The ride quality was quantified by measuring lateral acceleration from an inertial measurement sensor. The differences between the mean lateral acceleration for the VPS enabled system and the other modes of operation were under three thousandths of a G and the standard deviation differed by less than seven thousandths of a G, proving the ride quality between the modes of operation are virtually indistinguishable.

The haptic feedback through the steering wheel provides a level of automated lane keeping to the bus when the lane assist system is operating. The feedback is controlled by a PID steering controller within the lane assist system, which drives a servo motor connected to the steering wheel. The performance of the lane-keeping offers some insight into how the lane assistance system performs. Lateral offset data was collected during enhanced VPS enabled lane assistance operation of the bus to quantify the performance of the automated lane-keeping. 2,099 data points were collected over two trial runs on the university transitway from Minneapolis to St. Paul. The IV Lab research bus is 2.59 meters wide and operates in lanes as narrow as 3.05 meters. This leaves 0.23 meters on each side of the vehicle. Although the data shows that the lane boundary limits are at most 1 ½ standard deviations from the means described in Figure 36 and Figure 37, the lane boundaries are still crossed at times. This is assumed to happen not from the position errors in the enhanced VPS, but from sub-optimal steering controller performance. Increased performance can be obtained from automated lane-keeping by optimizing the steering controller.

Overall, the implementation of the VPS enabled IV Lab Lane Assistance System was shown to be successful since the in-lane (where in the lane) level position accuracy was within the

required level, the ride quality was indistinguishable from DGPS and manual operation, and the lane-keeping performance was adequate.

E. Recommendations for Further Research

Further improvements to the enhanced VPS can be made to increase the likelihood of large scale deployment on BRT systems. Procuring an RFID reader with a higher read frequency will increase the accuracy of the VPS updates by an order of magnitude (1.0 to 0.1 meter error at 50 mph). Optimizing the steering controller in the enhanced VPS enabled IV Lab lane assist system will allow for increased performance of automated lane-keeping and haptic feedback.

Further research could also be directed at increasing the accuracy and robustness of the LiDAR curb detector. The probability of false detections could be attenuated by more effective LiDAR data filtering. If data points that are not part of the curb can be predetermined and removed, the algorithm can be more robust and efficient. Also, it was assumed that vehicle roll had no effect of lateral position measurements from the LiDAR. This assumption has minimal effects if the vehicle roll angle is repeatable for a given location on the road, but if potholes or other exogenous factors induce vehicle roll angle, lateral position measurement errors could be significant. An IMU could be used to measure the vehicle roll induced by bumps, ruts, etc, and mitigate the lateral position errors due to this type of noise.

Perhaps the biggest hurdle that stands in the way of large scale deployment of the enhanced VPS is the requirement that the vehicle needs a clear view of a curb or other easily recognizable three dimensional reference structure, such as a guard rail or Jersey barrier. Currently, if anything blocks the line of sight of the curb (snow drifts, parked cars, etc.) or the vehicle is in an intersection or driveway, the enhanced VPS is inoperable. One possible solution may be to measure lateral position off of a building, light pole, etc. with a LiDAR unit when available, and then updating the vehicle's position with a two dimensional speed sensor for higher frequency estimates or when a reference structure is not available. One major advantage to this configuration is that the LiDAR sensor can be moved high enough to "look" over cars, people, and other obstacles in order to measure a lateral distance from a tall[20] structural reference, such as a building or light pole. This configuration would be less susceptible to obstacles interfering with the view of the structural reference. If a system like this were developed, it would make enhanced VPS a much more flexible and attractive system. Enhanced VPS could also be used in other applications, such as precision docking. The LiDAR curb detection algorithm can provide the lateral position accuracy needed for such an application.

[20] Meaning tall relative to a person, car, snow bank or other common obstruction

References

[1] D. Schrank, T. Lomax, "The 2007 Urban Mobility Report", Texas A&M University System, Texas Transportation Institute, College Station, TX, September 2007.

[2] L. Alexander, P. Cheng, M. Donath, A. Gorjestani, B. Newstrom, C. Shankwitz, W. Trach, "DGPS-based Lane Assist System for Transit Buses", *Proceedings of the IEEE Intelligent Transportation Systems Conference*, October 3-6, 2004.

[3] J. Crassidis, J. Junkins, *Optimal Estimation of Dynamic Systems*, Chapman & Hall/CRC, Boca Raton, FL, 2004, pp. 189-191.

[4] M. Bevilacqua, "Vehicle Positioning System Using RFID Technology and its Use in the Design of a Rear-end Collision Avoidance System", M.S. Thesis, University of Minnesota – Twin Cities, Minneapolis, MN, 2006.

[5] P. Cheng, M. Donath, A.Gorjestani, A. Menon, B. Newstrom, C. Shankwitz, "DGPS System Augmentation for Lane Assist in Urban Areas", *Proceedings of the 63rd Annual Meeting of the Institute of Navigation*, April 23-25, 2007, pp. 665-673.

[6] C. Chan, "Magnetic Sensing as a Position Reference System for Ground Vehicle Control", *IEEE Transactions on Instrumentation and Measurement*, February 2002.

[7] D. Pomerleau, T. Jochem, "Rapidly Adapting Machine Vision for Automated Vehicle Steering", *IEEE Expert*, April 1996, pp. 19-27.

[8] C. Yu, D. Zhang, "Road Curbs Detection Based on Laser Radar", *IEEE 8th International Conference on Signal Processing*, 2006.

[9] W. Wijesoma, K. Kodagoda, A. Balasuriya, "Laser and Vision Sensing for Road Detection and Reconstruction", *IEEE 5th International Conference on Intelligent Transportation Systems*, September 3-6, 2002.

[10] R. Wang, B. Gu, L. Jin, T. Yu, L. Gou, "Study on Curb Detection Method Based on 3D Range Image by LaserRadar", *IEEE Intelligent Vehicles Symposium*, June 2005.

[11] R. Aufrére, J. Gowdy, C. Mertz, C. Thorpe, C. Wang, T. Yata, "Perception for Collision Avoidance and Autonomous Driving", *Mechatronics*, Vol. 13, No. 10, December 2003, pp. 1149-1161.

[12] B. Douglas, J. Bencel, "Navigation System for Automatic Guided Vehicle", U.S. Patent 6,049,745, April 11, 2000.

[13] M. Marino,W. Ross, "Station Control System for a Driverless Vehicle", U.S. Patent 7,174,836, February 13, 2007.

[14] R. Cummings, A. Cummings, "Passive Traffic Lane Marking for On-board Detection of Lane Boundary", U.S. Patent 7,140,803, November 28, 2006.

[15] P. Nysen, “Environmental Location System”, U.S. Patent 6,259,991, July 10, 2001.

[16] K. Finkenzeller, *RFID Handbook: Fundamentals and Applications in Contactless Smart Cards and Identification*, 2nd edition, John Wiley & Sons, West Sussex, U.K., 2004.

[17] M. Sergi, B. Newstrom, A. Gorjestani, C. Shankwitz, M. Donath, “Dynamic Evaluation of High Accuracy Differential GPS”, *Proceedings of the 2003 National Technical Meeting of the Institute of Navigation*, January 22-24, 2003, pp. 581-592.

[18] Partners for Advanced Transit and Highways, *Magnetic Guidance System (MGS)*, April 1998, retrieved September 17, 2008, from http://www.path.berkeley.edu/PATH/Research/magnets/.

Appendix A

A.1 Curb Detection Algorithm

LiDAR scans are sent to the curb detector algorithm at 33 hz. The curb model, from the curb model table, is sequentially overlaid over each data point in the LiDAR scan. For every overlay, an aggregate error is computed and the location where the aggregate error is the lowest is chosen as the "best fit" location. Figure 38 shows a flowchart of this process.

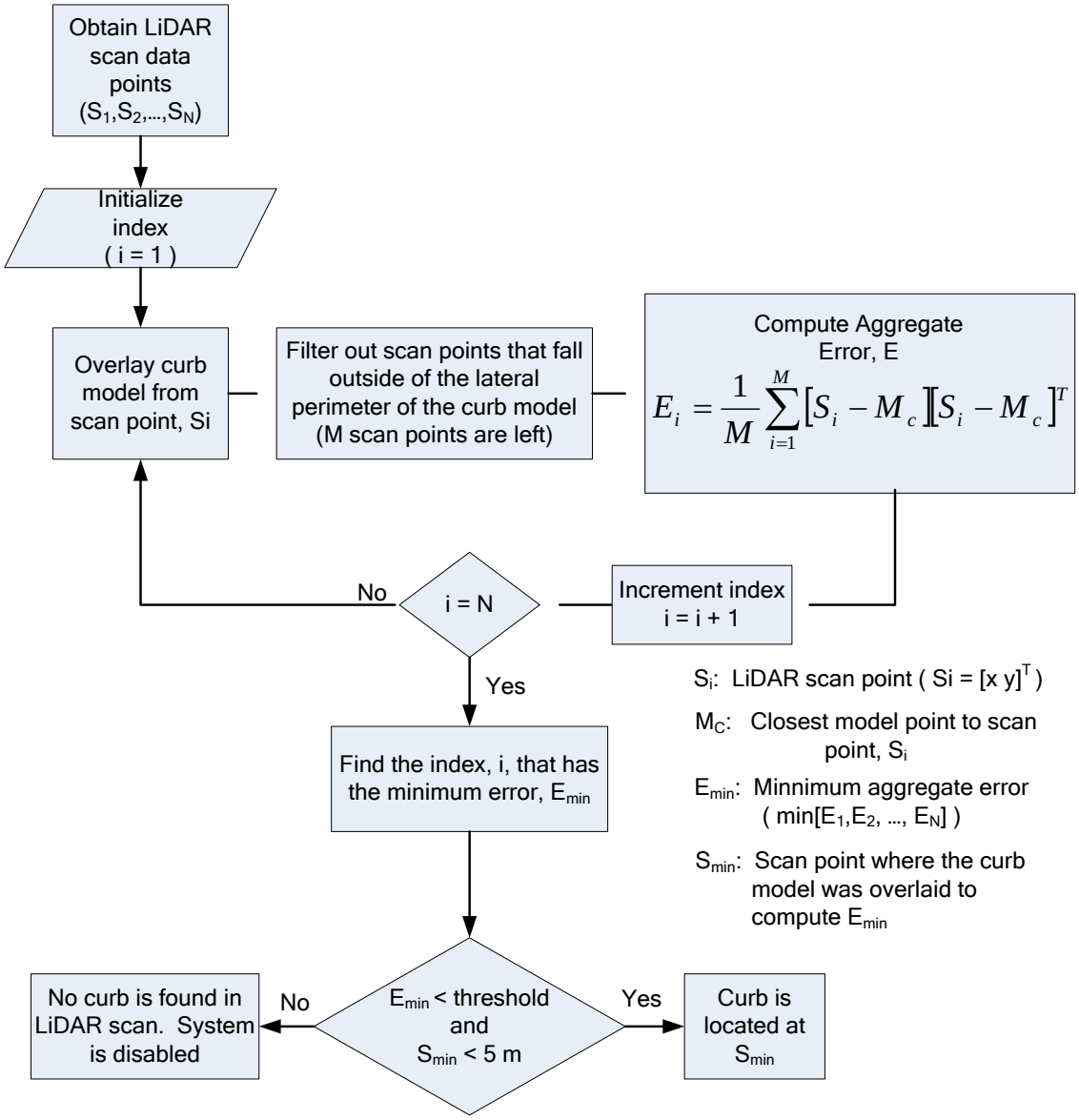

Figure 38. Flowchart of curb detection algorithm

A.2 Derivation of Lateral Position Error due to Road Curvature

Assumptions:

- Road curvature follows circular path

- x – Actual longitudinal position
- $\hat{x}$ – Longitudinal position measurement from VPS
- $\tilde{x}$ – Longitudinal position measurement error, ($\tilde{x} = x - \hat{x}$)
- $\tilde{y}$ -- Lateral position error induced by erroneous feedback from lane assist system
- m – Curb slope, $m = \Delta y/\Delta x$, as depicted in Figure 12 (can be thought of as the derivative of the distance from the curb to the lane center as a function of longitudinal position)
- r – Radius of curvature error, (r = smallest radius of curvature of the roadway)

The maximum lateral position error of the vehicle due to incorrect feed-forward steering angle information queried from the map database will follow the path of a circle of radius, *r*.

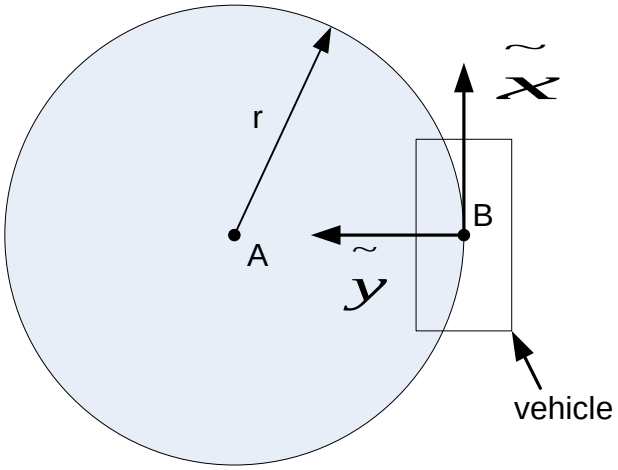

Figure 39. Derivation of lateral position error due to road curvature

$$\tilde{x}^2 + (r - \tilde{y})^2 = r^2 \quad \text{(Eq. 1)}$$

Equation 1 is an equation for a circle with the origin located at B. Solving equation 1 for $\tilde{y}$, yields,

$$\tilde{y} = r - \sqrt{r^2 - \tilde{x}^2} \quad \text{(Eq. 2)}$$

A.3 Histograms of Curb Detection Data Sets

Histograms of the LiDAR characterization data sets are shown in the following figures. Table 3 and

Table 4 in chapter three summarize the characteristics of the data sets.

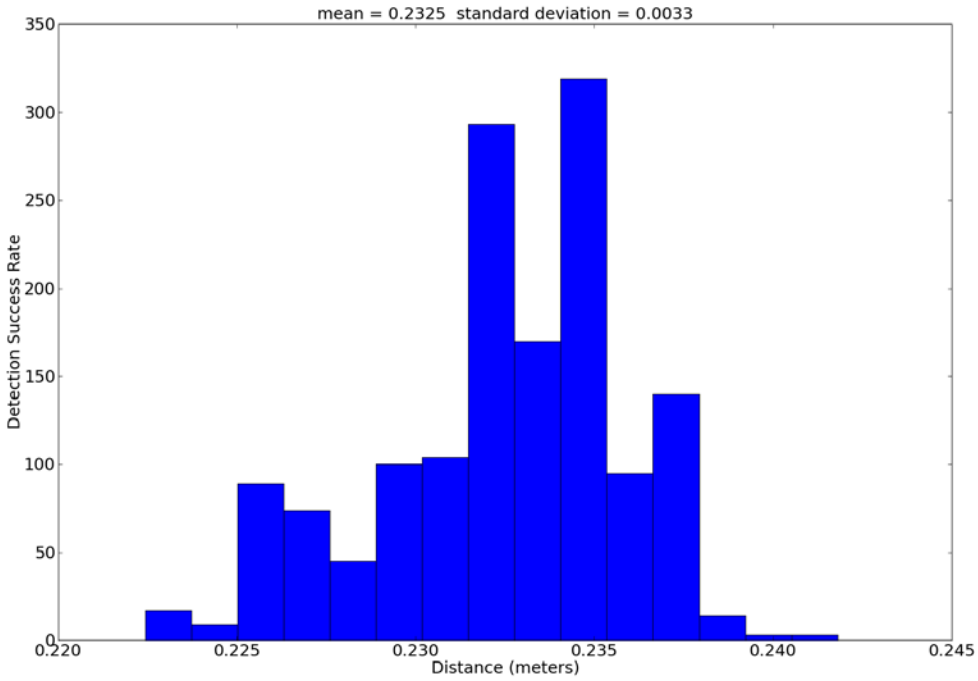

Figure 40. Trial 1

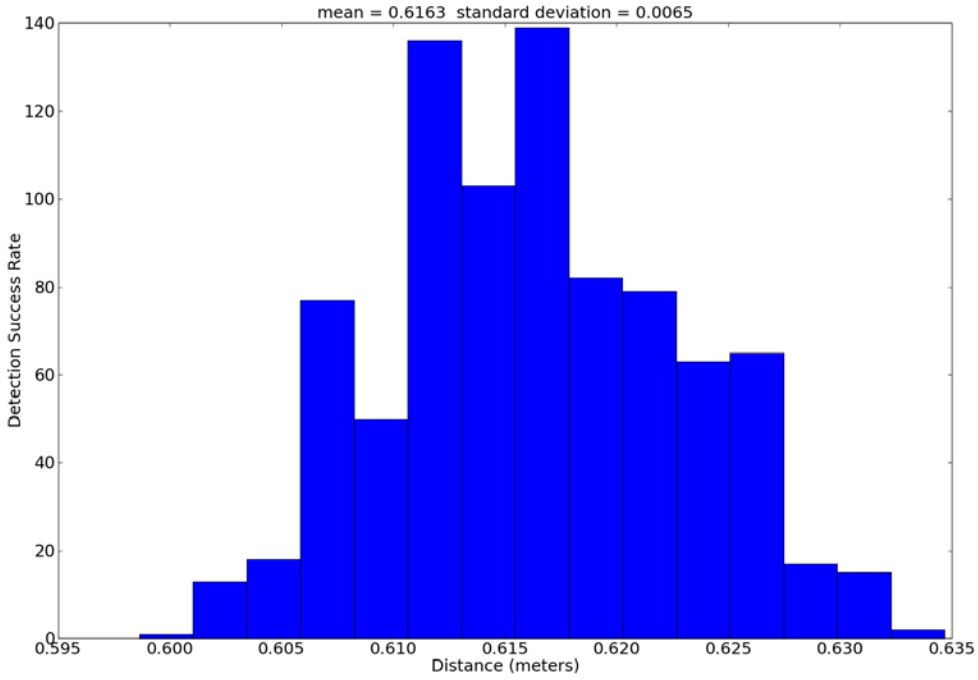

Figure 41. Trial 2

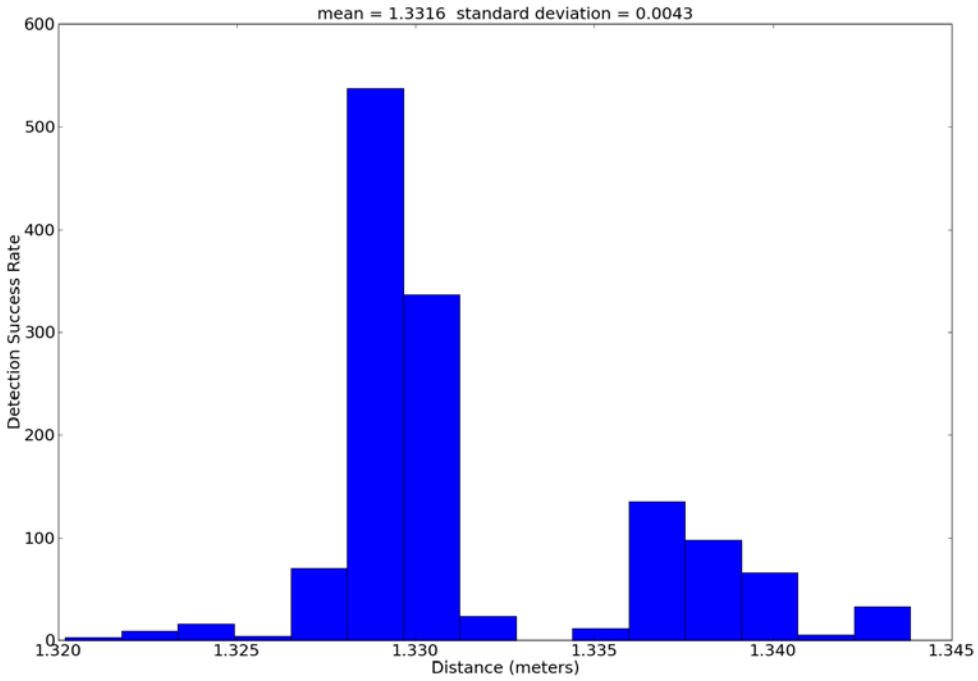

Figure 42. Trial 3

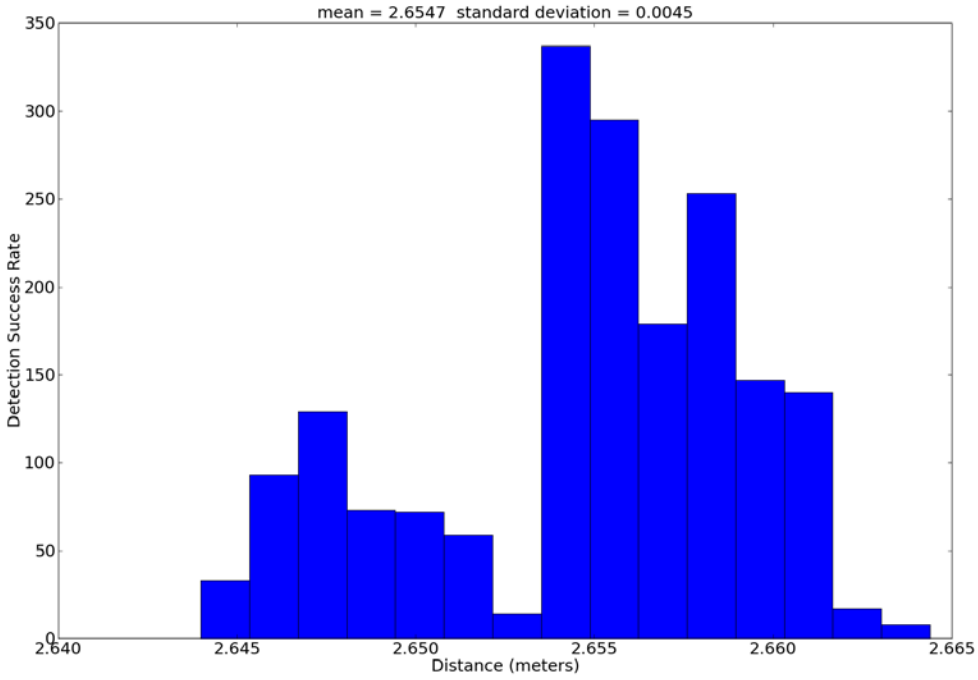

Figure 43. Trial 4

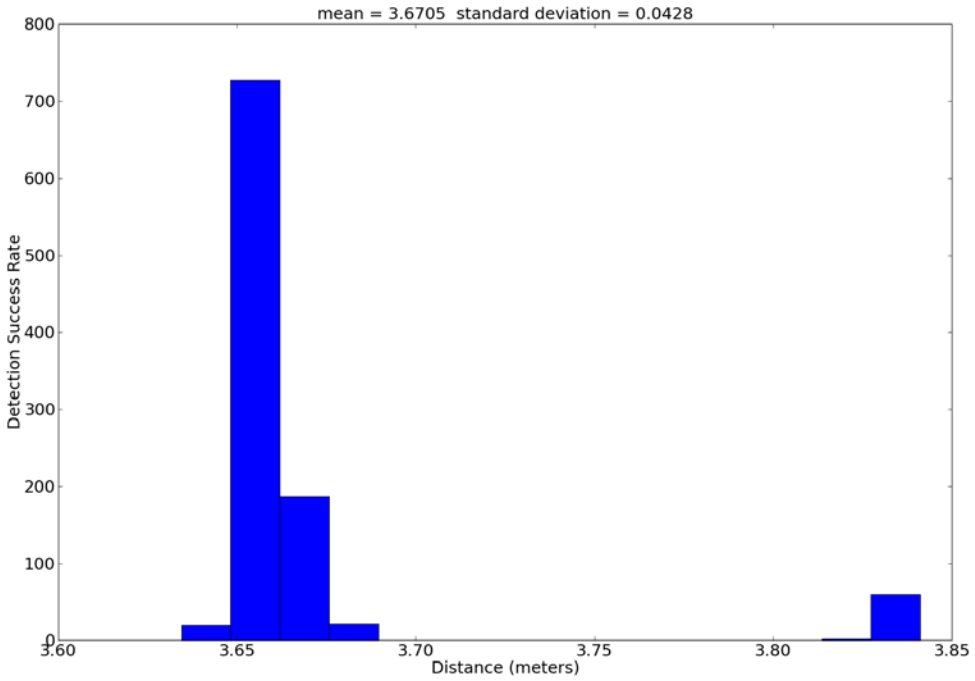

Figure 44. Trial 5

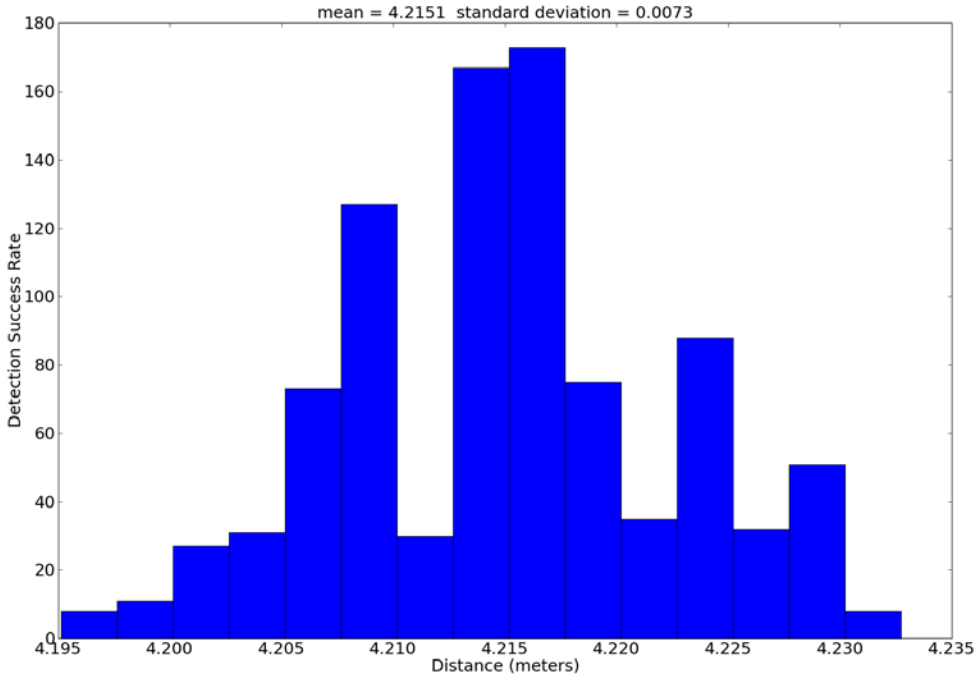

Figure 45. Trial 6

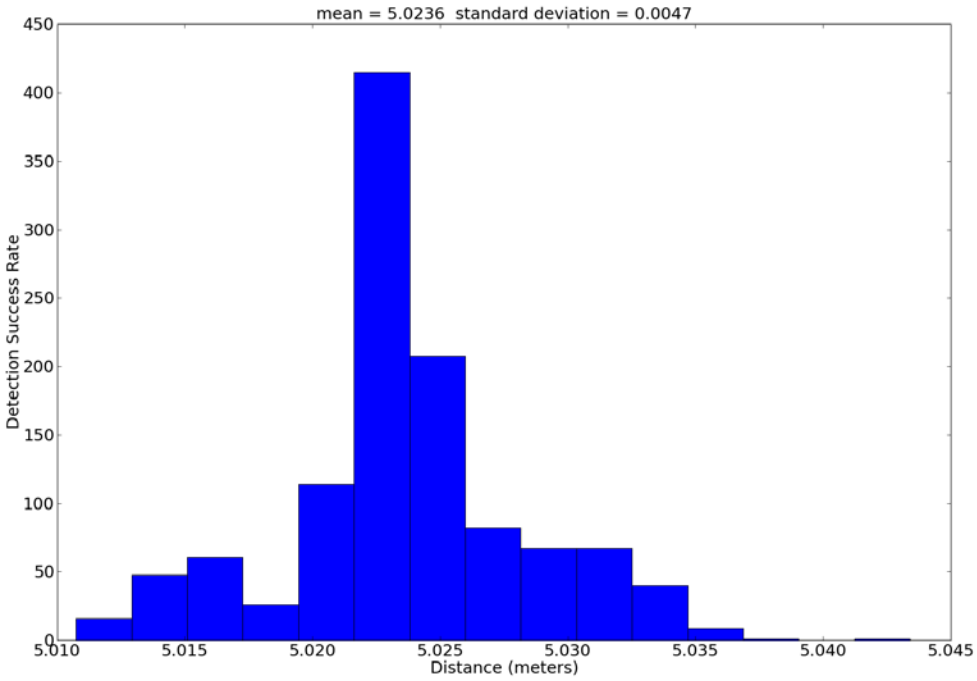

Figure 46. Trial 7

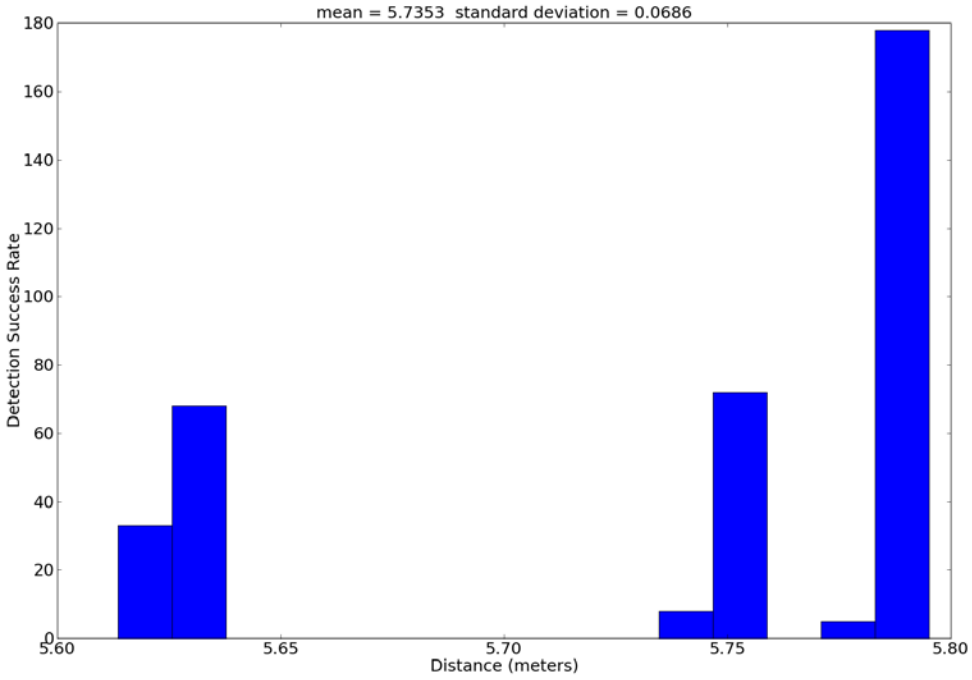

Figure 47. Trial 8

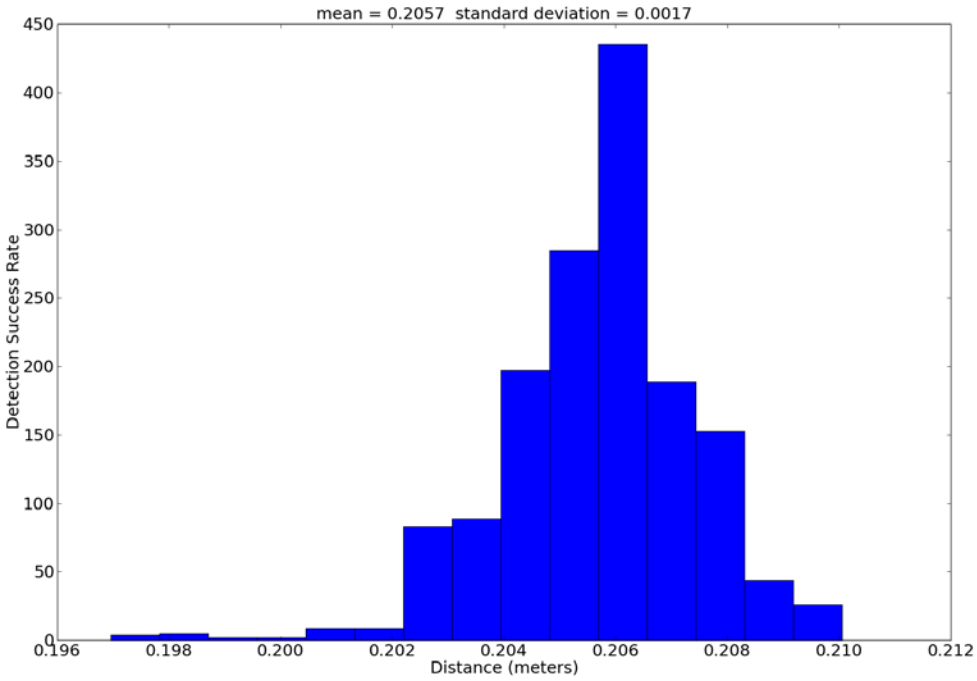

Figure 48. Trial 9

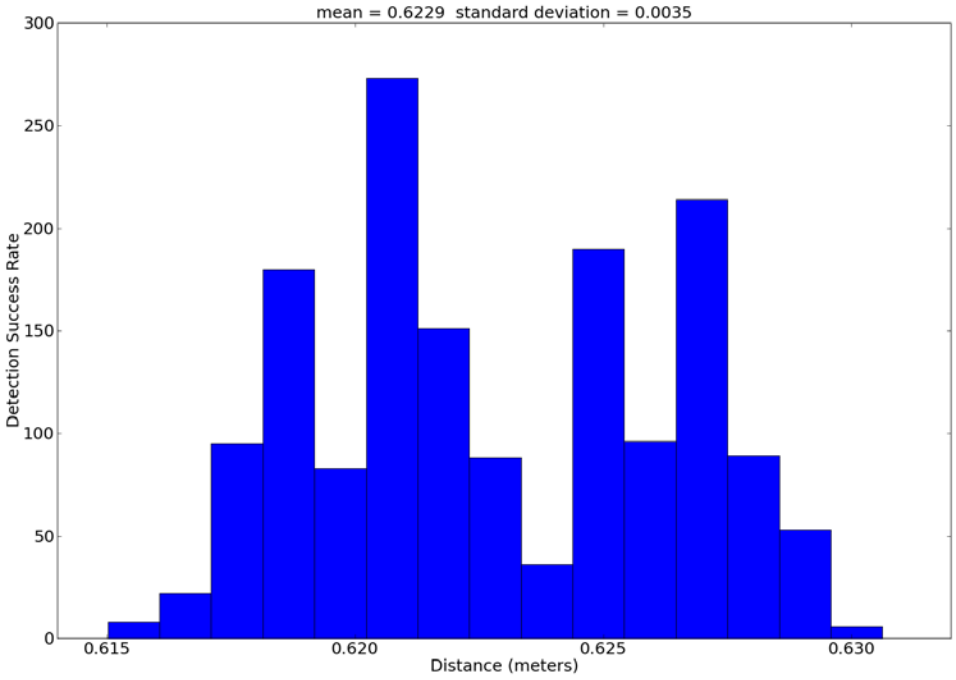

Figure 49. Trial 10

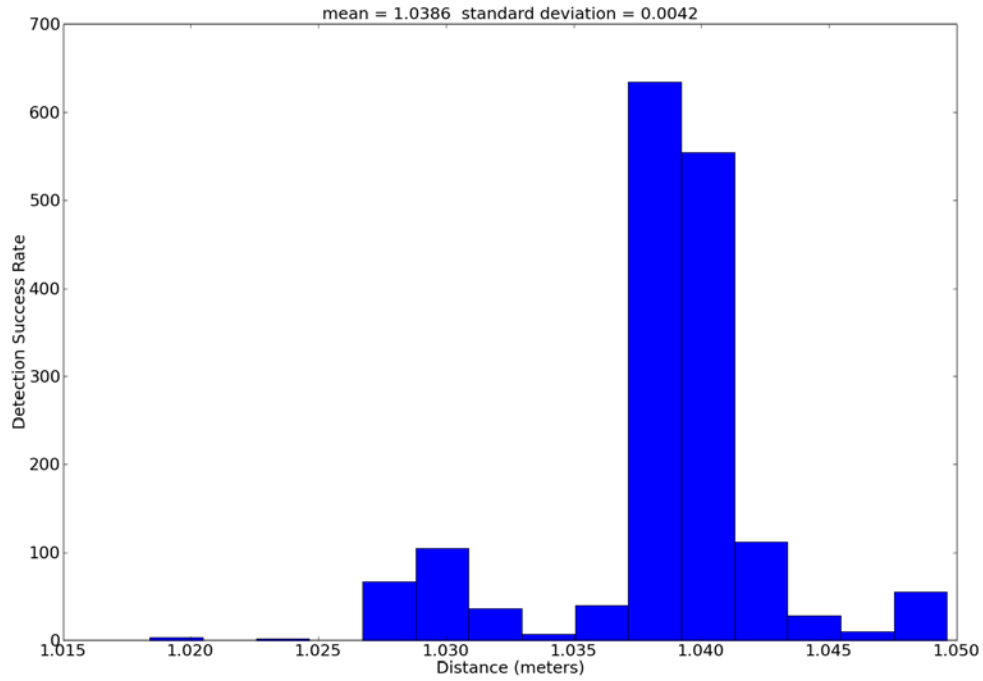

Figure 50. Trial 11

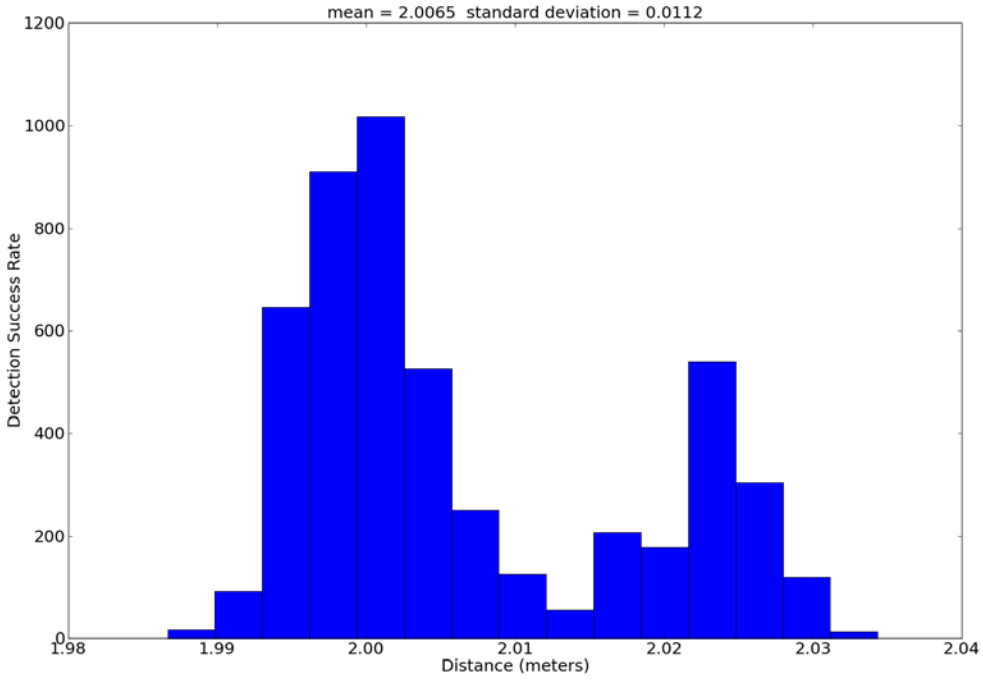

Figure 51. Trial 12

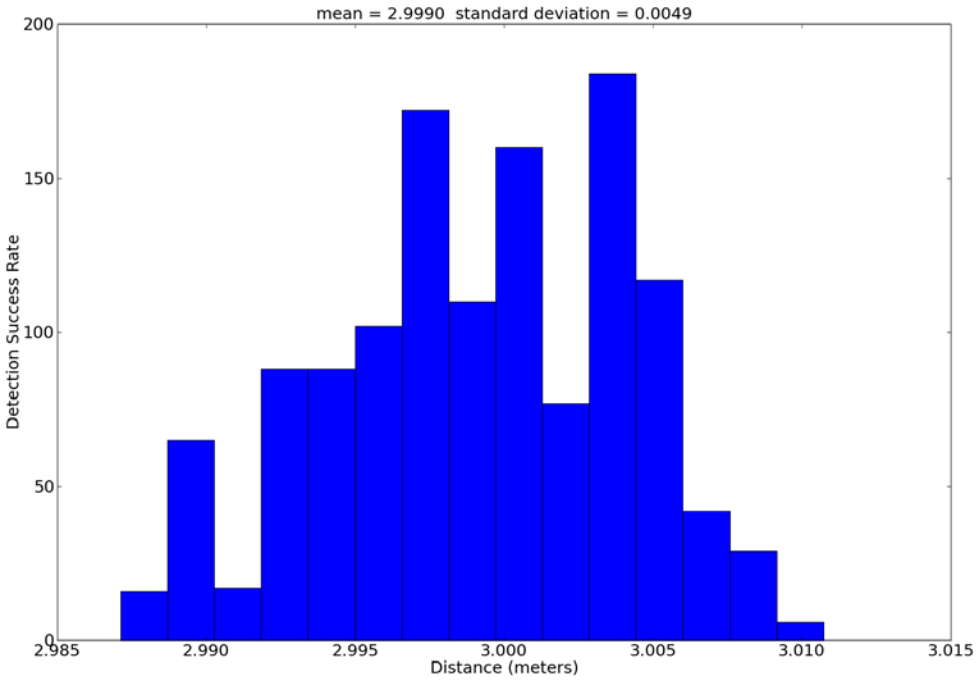

Figure 52. Trial 13

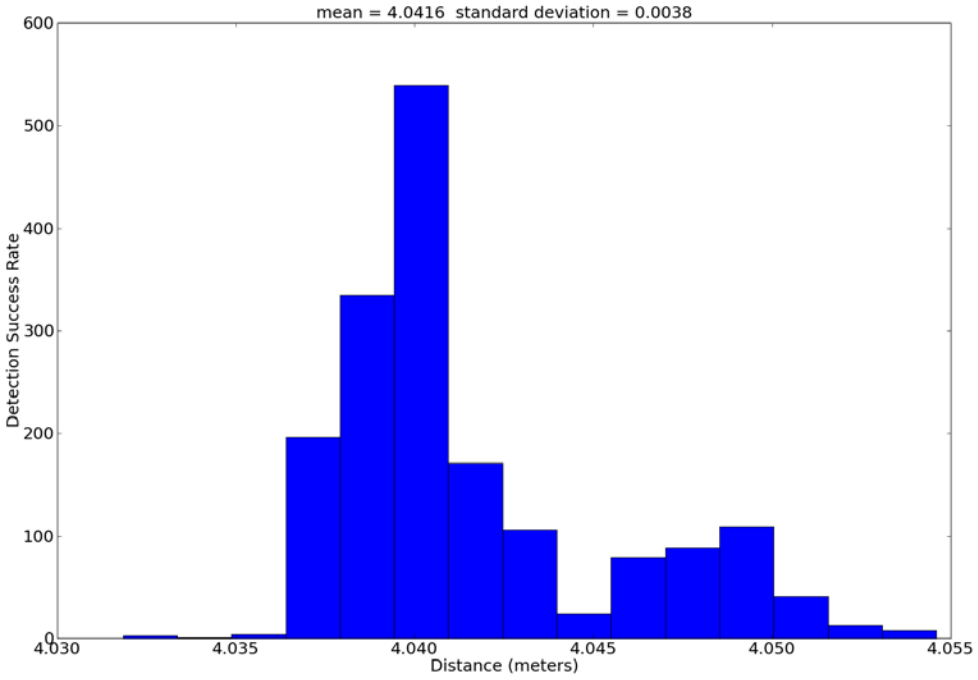

Figure 53. Trial 14

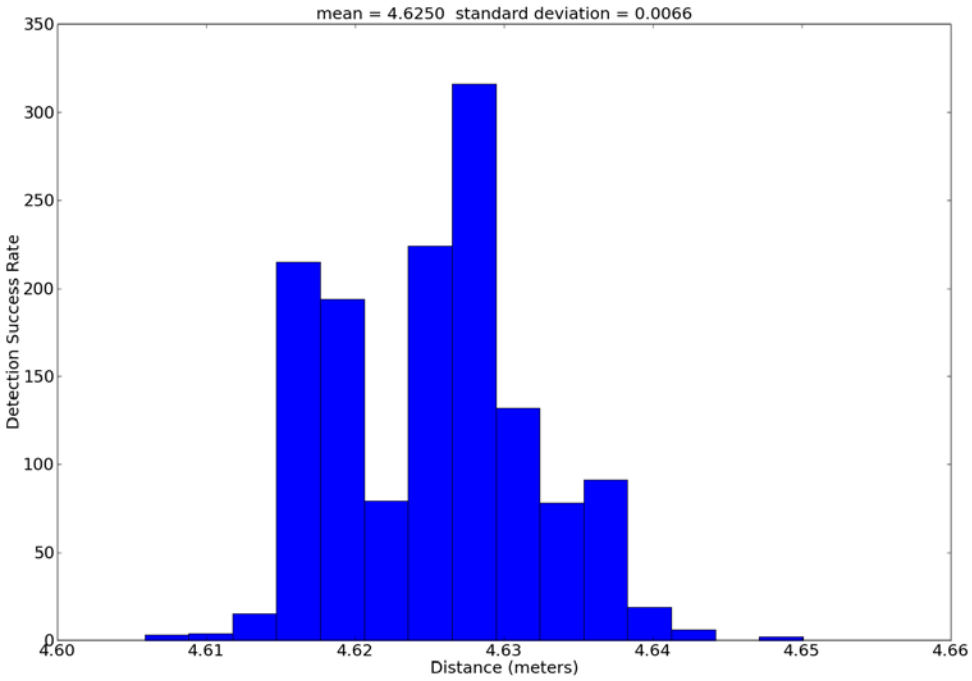

Figure 54. Trial 15

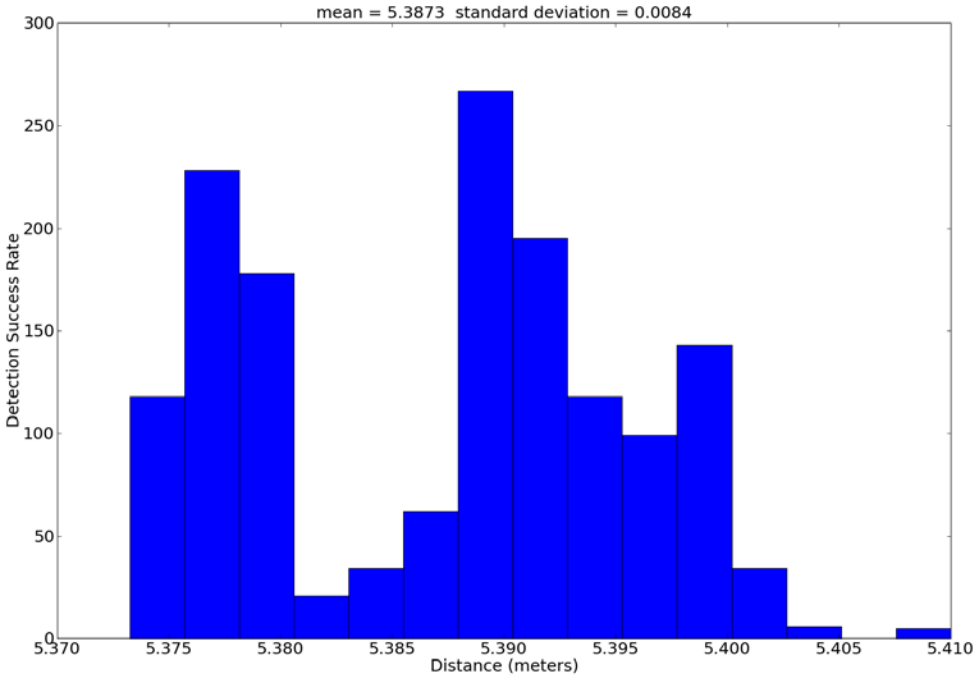

Figure 55. Trial 16

A.4 Computing DGPS Lateral Lane Offsets

DGPS position data was collected during the same mapping run (when the vehicle is assumed to drive down the center of the lane) used to derive the enhanced VPS map database. This ensures that the lateral offsets calculated from the VPS system and those post-processed from the DGPS position data are from the same lane center positions. The DGPS mapping data is illustrated in Figure 56. A subsequent trial run is then driven and DGPS position data is collected (trial run data points as shown in Figure 56). When each trial run data point is collected the associated lateral offset measured by the enhanced VPS is also collected. When the lateral offset is post-processed from the trial run data point and the DGPS mapping data, it is compared with the associated lateral offset measured by the enhanced VPS to determine the lateral error from the VPS offset measurement. The following describes how the lateral offset was post-processed from the DGPS data.

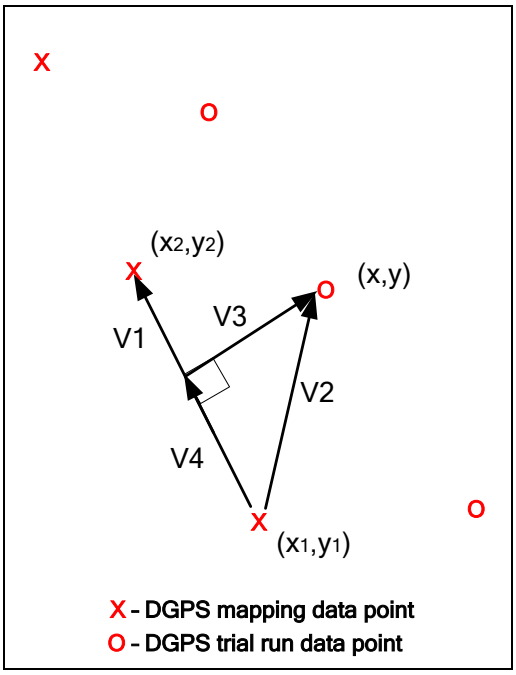

Figure 56. Computing DGPS lateral lane offsets

The lateral lane offset is defined as the perpendicular distance from the trial run data points to line segments constructed from the mapping data points. The following derives the formula of finding the perpendicular distance, $\overrightarrow{V_3}$, from a point, (x,y), to a vector, V_1.

$$\overrightarrow{V_1} = \begin{bmatrix} x2 - x1 \\ y2 - y1 \end{bmatrix}, \overrightarrow{V_2} = \begin{bmatrix} x - x1 \\ y - y1 \end{bmatrix}$$

$$\overrightarrow{V_3} = \frac{\overrightarrow{V_1} \times \overrightarrow{V_2}}{\left|\overrightarrow{V_1}\right|}$$

Point (x,y) is between (x_2,y_2) and (x_1,y_1) if,

$$0 \leq |\overrightarrow{V_4}| \leq |\overrightarrow{V_1}|$$

where,

$$|\overrightarrow{V_4}| = \frac{\overrightarrow{V_1} \cdot \overrightarrow{V_2}}{|\overrightarrow{V_1}|}$$

A.5 DRS1000 Specifications

Output	0-5 Volt square wave, differential, 100 Hz/MPH
Measurement Frequency	100 Hz.
Speed Measurement Range	1-300 MPH
Speed Measurement Error	$\pm(0.34\% + 0.0023\% \; per \; MPH)$
Microwave Characteristics	Frequency: Ka Band 35.5 GHz, +/- 0.1 GHz Beam Divergence Angle: 6^o from center Average RF Power: 0.02 W max Effective Radiated Power: 0.98 W
Power Supply	10.5 – 16.5 VDC, 2.4 W
Temperature Range	0-140^o F
Enclosure	Weather Resistant
Weight	0.5 lb.

A.6 WTPCT-M Frequency Counter Specifications

Table 8. Frequency counter specifications

Max input frequency	1.4 MHz
Resolution	5—digit (freq/period)
Accuracy	+/- 0.005%
Clock	20 MHz
Input Power	8 – 30 VDC
Current Draw	22 to 26 mA
Operating Temperature	0 – 70^{o} C
Dimensions	3.5 x 2.0 x 0.7 inches

A.7 Motorola Cargo RFID Tag Specifications

Table 9. Table of specifications for Motorola Cargo RFID tag (see www.motorola.com for detailed specs)

Dimensions	6 x 6 x 0.53 in. (H x W x D)
Tag Life	Up to five years
Weight	9.8 oz.
Data retention	Life of product
Memory	96 bit
Operating frequency	UHF band, 860 – 960 MHz
Polarization	Wide beam, polarization diverse
RF air protocol	EPC Gen 2 Class 1
Read distance	Up to 40 ft.
Operating Temperature	-40 – 70^{o} C